



Fisheries and Oceans
Canada

Pêches et Océans
Canada

Ecosystems and
Oceans Science

Sciences des écosystèmes
et des océans

Canadian Science Advisory Secretariat (CSAS)

Research Document 2015/013

Québec Region

**Chemical and Biological Oceanographic Conditions in the Estuary and Gulf
of St. Lawrence during 2013**

L. Devine, S. Plourde, M. Starr, J.-F. St-Pierre, L. St-Amand,
P. Joly and P. S. Galbraith

Fisheries and Oceans Canada
Maurice Lamontagne Institute
850 de la Mer, P. O. Box 1000
Mont-Joli, QC, G5H 3Z4

Foreword

This series documents the scientific basis for the evaluation of aquatic resources and ecosystems in Canada. As such, it addresses the issues of the day in the time frames required and the documents it contains are not intended as definitive statements on the subjects addressed but rather as progress reports on ongoing investigations.

Research documents are produced in the official language in which they are provided to the Secretariat.

Published by:

Fisheries and Oceans Canada
Canadian Science Advisory Secretariat
200 Kent Street
Ottawa ON K1A 0E6

[http://www.dfo-mpo.gc.ca/csas-sccs/
csas-sccs@dfo-mpo.gc.ca](http://www.dfo-mpo.gc.ca/csas-sccs/csas-sccs@dfo-mpo.gc.ca)



© Her Majesty the Queen in Right of Canada, 2015
ISSN 1919-5044

Correct citation for this publication:

Devine, L., Plourde, S., Starr, M., St-Pierre, J.-F., St-Amand, L., Joly, P. and Galbraith, P. S. 2015. Chemical and Biological Oceanographic Conditions in the Estuary and Gulf of St. Lawrence during 2013. DFO Can. Sci. Advis. Sec. Res. Doc. 2015/013. v + 45 pp.

TABLE OF CONTENTS

ABSTRACT	iv
RÉSUMÉ.....	v
INTRODUCTION.....	1
METHODS	1
RESULTS	4
NUTRIENTS AND PHYTOPLANKTON	4
High-frequency monitoring sites	4
Sections and late winter helicopter survey.....	5
Remote sensing of ocean colour	5
ZOOPLANKTON	6
High-frequency monitoring sites	6
Gulf subregions	7
Copepod phenology	8
Scorecards	8
DISCUSSION.....	9
SUMMARY.....	12
ACKNOWLEDGEMENTS.....	13
REFERENCES.....	13
TABLE.....	16
FIGURES	17

ABSTRACT

An overview of chemical and biological oceanographic conditions in the Gulf of St. Lawrence in 2013 is presented as part of the Atlantic Zone Monitoring Program (AZMP). AZMP data as well as data from regional monitoring programs are analyzed and presented in relation to long-term means in the context of a strong warming event that began in 2010. Phytoplankton and zooplankton abundance indices and nutrient inventories were relatively coherent through the time series (1999–2013) between the high-frequency monitoring sites and among sections and subregions. Nutrient inventories returned to near-normal levels in 2013, ending the period of strong negative anomalies that was seen in 2010–2012. The strong spring freshet of the St. Lawrence River delayed the spring bloom in the Estuary and NW Gulf and also led to lower-than-normal abundances of *Calanus finmarchicus* and *C. hyperboreus*. Warmer temperatures overall are likely behind the shift to smaller phytoplankton (since 2004 at Rimouski station) and the lower-than-normal abundances of cold-water copepod species. Satellite images of ocean colour were coherent with field measurements of chlorophyll content, thus increasing our confidence in what these images revealed over larger spatial and temporal scales than were covered during sampling campaigns. Our results and independent evidence from ecosystem surveys indicate that the decreased abundance of large zooplankton might be due to a combination of detrimental environmental conditions (bottom-up processes) and an increase in predation pressure (top-down processes).

Les conditions océanographiques chimiques et biologiques dans l'estuaire et le golfe du Saint-Laurent en 2013

RÉSUMÉ

Un aperçu des conditions océanographiques chimiques et biologiques dans le golfe du Saint-Laurent en 2013 est présenté dans le cadre du Programme de Monitoring de la Zone Atlantique (PMZA). Les données du PMZA, ainsi que des données provenant de programmes de monitoring régionaux, sont analysées et présentées par rapport à des climatologies à long terme dans le contexte d'un événement de fort réchauffement qui a débuté en 2010. Les indices d'abondance pour le phytoplancton et le zooplancton ainsi que les inventaires de sels nutritifs étaient relativement cohérents à travers les séries temporelles (1999–2013) entre les stations fixes, les transects et les diverses régions. Les inventaires de sels nutritifs sont revenus à des niveaux près de la normale en 2013, mettant fin à la période de fortes anomalies négatives de 2010–2012. La forte crue printanière du fleuve Saint-Laurent a retardé la floraison printanière dans l'estuaire et le nord-ouest du golfe et a conduit à des abondances de *Calanus finmarchicus* et *C. hyperboreus* plus faibles que les normales. Des températures globalement plus élevées sont probablement la cause du passage vers du plus petit phytoplancton (depuis 2004 à la station Rimouski) et de la plus faible abondance que normale des espèces de copépodes d'eau froide. Les images satellitaires de la couleur de l'océan étaient cohérentes avec les mesures de chlorophylle faites sur le terrain, augmentant ainsi notre confiance en ce que les images ont révélé sur des échelles spatiales et temporelles plus grandes que celles couvertes pendant les campagnes d'échantillonnage. Nos résultats, ainsi que des observations indépendantes provenant du relevé écosystémique, suggèrent que le déclin de l'abondance du gros zooplancton pourrait être dû à une combinaison de conditions environnementales défavorables (processus «ascendants») et à une augmentation de la pression de prédation (processus «descendants»).

INTRODUCTION

The Atlantic Zone Monitoring Program (AZMP) was implemented in 1998 (Therriault et al. 1998) with the aim of (1) increasing Fisheries and Oceans Canada's (DFO) capacity to understand, describe, and forecast the state of the marine ecosystem and (2) quantifying the changes in the ocean's physical, chemical, and biological properties and the predator–prey relationships of marine resources. A critical element in the observational program of AZMP is an annual assessment of the distribution and variability of nutrients and the plankton they support.

A description of the spatiotemporal distribution of nutrients (nitrate, silicate, phosphate) and oxygen dissolved in seawater provides important information on water-mass movements and on the locations, timing, and magnitude of biological production cycles. A description of the distribution of phytoplankton and zooplankton provides important information on the organisms forming the base of the marine food web. An understanding of plankton production cycles is an essential part of an ecosystem approach to fisheries management.

The AZMP derives its information on the state of the marine ecosystem from data collected at a network of sampling locations (high-frequency monitoring sites, cross-shelf sections) in each DFO region (Québec, Gulf, Maritimes, Newfoundland; see Fig. 1 for Québec region locations) sampled at a frequency of weekly to once annually. The sampling design provides basic information on the natural variability in physical, chemical, and biological properties of the Northwest Atlantic continental shelf: cross-shelf sections provide detailed geographic information but are limited in their seasonal coverage while critically placed high-frequency monitoring stations complement the geography-based sampling by providing more detailed information on temporal (seasonal) changes in ecosystem properties.

In this document, we review the chemical and biological oceanographic (lower trophic levels) conditions in the Gulf of St. Lawrence (GSL) in 2013. While surface and deep composite water temperatures decreased in 2013 relative to the highly anomalous warm conditions observed in 2012, temperatures remained well above the long-term average in 2013, a situation that has persisted since 2010 (Galbraith et al. 2014). This report describes changes in the annual production cycles and community composition of phytoplankton and zooplankton in this context.

METHODS

All sample collection and processing steps meet and often exceed the standards of the AZMP protocol (Mitchell et al. 2002). All data included in this report were collected along seven sections during surveys done in June and October–November of each year and at two high-frequency monitoring sites (also called “fixed stations”; Fig. 1). Table 1 and Figure 2 show the 2013 surveys and the effort at high-frequency sampling sites, respectively. Those familiar with AZMP will note that the formerly designated Québec Region fixed stations—the Gaspé Current and Anticosti Gyre—are not included in this report; they will no longer be included as high-frequency sites but continue to be sampled during section occupations. It was difficult to sample these stations on a regular basis, particularly in winter. Rimouski station has been sampled since 1991 as part of a research project—about weekly throughout the summer, less frequently in early spring and late fall, and never in winter (except for physical variables during the March helicopter survey). It has been included in AZMP's annual review of environmental conditions since 2004 (AZMP 2006). Recently, several analyses were performed that indicated good correlations and correspondences between the Gaspé Current/Anticosti Gyre stations and Rimouski station (P. Galbraith, S. Plourde, J. Chassé; unpublished data), and it was thus

decided that Rimouski station would be integrated into AZMP to represent conditions in the St. Lawrence Estuary and the northwest GSL.

Since 1996, a survey has been conducted of the winter surface mixed layer of the GSL in early to mid-March using a Canadian Coast Guard helicopter; surface nutrients (2 m) were added to the sampling protocol in 2001 (Galbraith 2006, Galbraith et al. 2006). This survey has added a considerable amount of data to the previously sparse winter sampling in the region. A total of 107 stations were sampled during the 5–14 March 2013 survey. The temperature and salinity of the 2013 mixed layer are described by Galbraith et al. (2014).

Near-surface phytoplankton biomass was estimated from ocean colour data collected by the Sea-viewing Wide Field-of-view Sensor ([SeaWiFS](#)) satellite launched by NASA in late summer 1997 and by the Moderate Resolution Imaging Spectroradiometer ([MODIS](#)) “Aqua” sensor launched by NASA in July 2002. Because the SeaWiFS mission ended in December 2010, we present here the MODIS data obtained continuously from January 2003 until December 2013 to construct composite time series of surface chlorophyll *a* in six GSL subregions (Anticosti Gyre, Magdalen Shallows, Shediac Valley, Cabot Strait, northwest and northeast GSL; see Fig. 3 for locations). All selected subregions are located outside of the St. Lawrence River plume because data in regions influenced by this freshwater are unreliable due to turbidity and riverine input of terrestrially derived coloured matter. Composite satellite images were provided by BIO’s remote sensing unit (Bedford Institute of Oceanography, DFO, Dartmouth, NS) in collaboration with NASA GSFC (Goddard Space Flight Center). Basic statistics (mean, range, standard deviation) are extracted from two-week average composites with a 1.5 km spatial resolution. Seven different metrics were computed: the timing of spring bloom start and peak (day of year); the magnitude of the spring bloom (maximum chlorophyll *a*); the mean chlorophyll biomass during spring (March to May), summer (June to August), and fall (September to December) as well as its annual average (March to December). In addition, we computed normalized annual anomalies (see below) for each of the different bloom metrics to evaluate evidence of temporal trends among the different statistical subregions.

Chlorophyll and nutrient data collected along the AZMP sections and at fixed stations were integrated over various depth intervals (i.e., 0–100 m for chlorophyll; 0–50 m and 50–150 m for nutrients) using trapezoidal numerical integration. The surface (0 m) data were actually the shallowest sampled values; data at the lower depths were taken as either i) the interpolated value when sampling was below the lower integration limit or ii) the closest deep-water sampled value when sampling was shallower than the lower integration limit. Integrated nitrate values from the helicopter survey were calculated using surface concentrations (2 m) × 50 m; it was assumed that the nitrate concentrations are homogeneous in the winter mixed layer at that time of the year.

Some zooplankton data collected in 2001 along the AZMP sections that had been excluded from the previous analysis due to serious doubts about the quality of the analysis were re-analyzed in 2013–2014 and are incorporated into this report. Because of this and also due to some minor modifications to the query extracting data from the database (e.g., we had been missing one *Pseudocalanus* spp. stage category from Shediac Valley station), some of the time series results in the present report may differ slightly from previously published reports.

In this document, we give a detailed description of the seasonal patterns in zooplankton indices for Rimouski and Shediac Valley stations. In recent years, the number and type of zooplankton indices as well as the way they are reported have been rationalized with the aim of standardizing research documents among AZMP regions. We thus present total zooplankton biomass, total copepod abundance, relative contribution of the 10 most abundant copepod species, and *C. finmarchicus* and *Pseudocalanus* spp. (Rimouski station only) abundance and

stage composition for the high-frequency monitoring sites. Because of its importance to the total zooplankton biomass in the region, a detailed description of *C. hyperboreus* was added. We present the spring and fall total zooplankton biomass and total abundance of *C. finmarchicus*, *C. hyperboreus*, and *Pseudocalanus* spp. for three regions having distinct oceanographic regimes (identified by different colours in Fig. 1) and corresponding more to the spatial scales addressed by AZMP in other regions (Koutitonsky and Budgen 1991, Galbraith et al. 2013):

- (1) western GSL (wGSL): this region is generally deep (> 200 m) and cold in summer. It is strongly influenced by freshwater runoff from the St. Lawrence River and cold and dense waters from the Laurentian Channel;
- (2) southern GSL (sGSL): this region is shallow (< 100 m) and much warmer in summer. It is under the influence of the Gaspé Current;
- (3) eastern GSL (eGSL): this region, with deep channels and a relatively wide shelf (< 100 m), is characterized by higher surface salinity and is directly influenced by the intrusion of water from the Labrador and Newfoundland shelves.

Standardized anomalies of key chemical and biological indices were computed for the high-frequency sampling stations, sections, and oceanographic regions. These anomalies are calculated as the difference between the variable's average for the season (i.e., chlorophyll and nutrient indices) or for the complete year (i.e., zooplankton indices) and the variable's average for the reference period (usually 1999–2010); this number is then divided by the reference period's standard deviation. Only actual measurements were used for these calculations, not modelled data. These anomalies thus represent observations in a compact format. A standard set of indices representing anomalies of nutrient availability, phytoplankton biomass and bloom dynamics, and the abundance of dominant copepod species and groups (*C. finmarchicus*, *Pseudocalanus* spp., total copepods, and total non-copepods) are produced for each AZMP region (see DFO 2013). We also present several zooplankton indices that reflect either different functional groups with different roles in the ecosystem or groups of species indicative of cold- or warm-water intrusions and/or local temperature conditions: large calanoids (dominated by *Calanus* and *Metridia* species), small calanoids (dominated by more neritic species such as *Pseudocalanus* spp., *Acartia* spp., *Temora longicornis*, and *Centropages* spp.), cyclopoids (dominated by *Oithona* spp. and *Triconia* spp.; the latter is a poecilostomatoid that is included in this category because of its ecological characteristics), warm-water species (*Metridia lucens*, *Centropages* spp., *Paracalanus* spp., and *Clausocalanus* spp.), and cold/arctic species (*Calanus glacialis* and *Metridia longa*).

Potential changes in zooplankton phenology were explored using *C. finmarchicus* as an indicator. We used the time series at Rimouski station because adequate sampling and stage identification started there 20 years ago (1994). From 1994 to 2004, *C. finmarchicus* copepodite stage abundance was determined using samples collected with 333 μm (CIV–CVI) and 73 μm (CI–III) mesh nets that were analyzed for seven years of the time series (see Plourde et al. 2009 for details). In other years before 2004 for which 73 μm samples were not analyzed, the abundance of CI–III in the 333 μm samples was adjusted based on a comparison done with an AZMP-like net (S. Plourde, unpublished data). The phenology of *C. finmarchicus* was described using the normalized (x/x_{max}) relative stage proportions of CI–III, CIV, CV, and CVI (male and female).

RESULTS

NUTRIENTS AND PHYTOPLANKTON

Distributions of the primary dissolved inorganic nutrients (nitrate, silicate, phosphate) included in AZMP's observational program strongly co-vary in space and time (Brickman and Petrie 2003). For this reason and because the availability of nitrogen is most often associated with phytoplankton growth limitation in coastal waters of the GSL, emphasis in this document is placed on variability in nitrate concentrations and inventories.

High-frequency monitoring sites

The Rimouski and Shediac Valley stations typically exhibit a biologically mediated reduction in surface nitrate concentrations in spring/summer, a minimum during summer, and a subsequent increase during fall/winter (Fig. 4). The onset of the nutrient draw-down occurs later at Rimouski station compared to Shediac Valley station, reflecting the later spring bloom in the St. Lawrence Estuary (June) compared to Shediac Valley (April). In contrast to Shediac Valley station, surface nutrient inventories at Rimouski station remain relatively high during summer and usually at levels non-limiting for phytoplankton growth. These high levels are mainly due to upwelling at the head of the Laurentian Channel and the high tidal mixing in this area, and to some degree to anthropogenic and river sources, notably from the St. Lawrence River.

In 2013, the nutrient draw-down occurred more gradually at Rimouski station, reaching its lowest value at the end of the sampling season in September–October (Fig. 4). We also saw the lowest chl *a* concentrations of the season in June—usually when the bloom is highest—while the maximum chl *a* biomass was observed in August and September. This August–September peak was also seen in 2012, although there had already been the typical strong June peak. When averaged for the entire sampling period, both chlorophyll and nitrate inventories were nevertheless close to the 1999–2010 average.

The early spring bloom at Shediac Valley station was not captured by the 2013 sampling. Nevertheless, evidence of a bloom is seen in the drop in nitrate concentration between the March helicopter survey and the first ship-based sampling in April. Nitrate and chl *a* levels at that station were generally close to the 1999–2010 mean, although there was no evidence of the secondary bloom seen in the 1999–2010 time series in October, when the 2013 sampling season ended.

Diatom and dinoflagellate abundances were below the long-term average at Rimouski station, as they have been since 2011, but flagellate abundances returned from below to near normal (Fig. 5). While the phytoplankton community was regularly dominated by diatoms throughout the sampling period between 1999 and 2003, a shift from diatoms towards flagellates and dinoflagellates has been observed since 2004 (Fig. 5). In 2013, the predominance of flagellates was stronger than it had been since 2008 while the diatom/dinoflagellate ratio was close to the 1999–2010 reference period average (Fig. 5). The seasonal pattern of the major phytoplankton groups was very different from the reference period due to a sharp decrease in the relative contribution of diatoms in June and a decrease in August that was stronger than usual (Fig. 6).

Dinoflagellate and flagellate abundances at Shediac Valley station were below the long-term averages while that of diatoms was somewhat above average for the first time since 2008 (Fig. 7). The seasonal evolution of the phytoplankton community composition in 2013 was broadly similar to the 1999–2010 reference period, with diatoms dominating in July–August and flagellates and dinoflagellates becoming increasingly important in the fall (Fig. 6).

Sections and late winter helicopter survey

Late winter nitrate inventories in 2013 were relatively high at the surface for most regions of the GSL except for unusually low ($<2 \text{ mmol m}^{-3}$) concentrations at some stations in the eastern part of the southern GSL (Fig. 8). These atypical low levels in the southern GSL, which were also observed in 2012, are probably due to an unusual localized start of phytoplankton growth at that time of the year; this is also seen in the satellite ocean colour data (Fig. 9). The highest winter surface nitrate concentrations were observed in the St. Lawrence Estuary, as in previous years, and concentrations gradually decreased from west to east. Transport of nutrient-rich water from the Estuary towards the southern GSL was clearly evident at that time of the year. The winter maximum nutrient inventories in 2013 returned to near normal values (i.e., the 2001–2010 average; Fig. 10, 11), ending the period of strong negative anomalies that was evident in 2010–2011 and to a lesser extent in 2012.

Late spring surface nitrate inventories in 2013 were low compared to late winter inventories along the seven sections crossing the Estuary and GSL due to utilization by phytoplankton (Fig. 12). Fall surface nitrate levels in 2013 were similar to or slightly higher than those measured during the late spring survey for all areas except for the estuarine portion of the GSL. This indicates that the autumnal turnover had not occurred or had just begun in many regions. The continued low nitrate level in the Estuary may be indicative of a fall phytoplankton bloom: although confirmation of this was not captured during concurrent chlorophyll sampling (Fig. 13), there was evidence of a stronger-than-average bloom in August–September at Rimouski station (Fig. 4).

The late spring nitrate inventories in 2013 were mostly above the 1999–2010 reference period averages after having been strongly negative since 2010 (Fig. 11); this is particularly true for the Estuary as well as the northwestern and central parts of the Gulf. This suggests that spring primary production may have been lower than usual. The differences between the winter maximum inventories and the late spring minimum inventories along the sections were variable but mostly near or below average, similar to what was seen in 2012. This index represents the pool of nutrients that was potentially used by phytoplankton during spring. A negative index indicates lower new phytoplankton production with potential detrimental effects on higher trophic levels. Similarly, the 2013 fall surface nitrate inventories were mostly near or slightly below the 1999–2010 mean. Examination of the standardized scorecard anomalies reveals that overall the nitrate inventories were predominantly above the 1999–2010 averages while chlorophyll concentrations were near or below the averages, especially in the Estuary and northwestern GSL (Fig. 11). This is consistent with data from Rimouski station. In contrast, deep nitrate inventories, particularly those below 200 m, were well above normal in the GSL in 2013 (Fig. 11).

Remote sensing of ocean colour

Satellite ocean colour data provide large-scale images of surface phytoplankton biomass (chlorophyll *a*) over the whole NW Atlantic. We used two-week satellite composite images of GSL subregions to supplement our ship-based observations and provide seasonal coverage and a large-scale context over which to interpret our survey data. The ocean colour imagery provides information about the timing and spatial extent of the spring and fall blooms but does not provide information on the dynamics that take place below the top few metres of the water column. In addition, satellite ocean colour data for the St. Lawrence Estuary are largely contaminated by high concentrations of nonchlorophyllous matter originating from the continent (such as suspended particulates and coloured dissolved organic matter) that render these data too uncertain to be used. Knowledge of phytoplankton dynamics in the St. Lawrence Estuary

and the subsurface information are gathered using the high-frequency sampling at Rimouski station and the broad-scale oceanographic surveys.

Satellite images in 2013 revealed considerable spatial variability in the timing of the spring bloom in the GSL (Fig. 14), as has been previously observed (not shown), which may be due to subregional differences in the timing of sea-ice melt and the onset of water column stratification (Le Fouest et al. 2005). The spring phytoplankton bloom occurred between March and May, depending on the region, and started earlier in the northwest and southern parts of the GSL (Fig. 14). The MODIS imagery confirmed the initiation of the spring bloom in the southern part of the GSL at the end of the helicopter survey in 2013 (Fig. 9); this likely explains the exceptionally low nitrate levels in this region at that time of the year (Fig. 8). The imagery also confirmed the overall low surface chlorophyll levels observed during our late spring and fall surveys during 2013 (Fig. 13, 15). A strong positive chlorophyll anomaly was revealed by satellite images in the southern GSL in late July (Fig. 16), but we have no concurrent shipboard sampling for this period. Satellite images show that fall blooms in the GSL are lower in magnitude than spring blooms; this was true for 2013 (Fig. 17), although lower-than-average fall values were seen in the western regions (Anticosti Gyre / NWGSL) and higher-than-average fall values were noted at Shediac Valley.

MODIS satellite observations from the six GSL subregions have shown a general trend toward the earlier timing of surface blooms, but this seems to have attenuated somewhat in 2013 (Fig. 17), with blooms of lower intensity that persist longer in most subregions. The standardized scorecard anomalies inferred from the MODIS satellite imagery showed some interesting patterns across the statistical subregions (Fig. 18). Anomalies of the mean annual surface chlorophyll and the spring bloom magnitude were similar from 2011–2013 while anomalies in the mean surface chlorophyll in June–August and September–December were comparatively higher in 2013. This indicates that while the shift to earlier timing of the spring bloom—which has been especially evident in the increased frequency of negative anomalies since 2010 across many of the subregions—is still occurring, chlorophyll levels during summer and fall have increased compared to recent years (2010–2012), except for the northwestern GSL.

ZOOPLANKTON

High-frequency monitoring sites

The long-term (Rimouski: 2005–2010; Shediac Valley: 1999–2010) seasonal climatologies of zooplankton biomass at the high-frequency monitoring stations are shown along with observations made in 2013 in Figure 19. The zooplankton biomass at Rimouski station in 2013 was generally above average early in the season, slightly below average in summer, and mostly above the long-term seasonal average starting in late July (Fig. 19a). At Shediac Valley station, zooplankton biomass was lower than normal from May through September 2013, with the exception of a single high value in late May, and near normal later in the season (Fig. 19b). However, results at this site must be considered carefully due to the low sampling frequency.

Total copepod abundance at Rimouski station in 2013 was near or slightly below normal from April to late August but generally above average in fall (Fig. 20a). This higher-than-normal abundance of copepods in September–October corresponded to a higher-than-normal proportion of *Microcalanus* spp., while the spring–summer period was mainly characterized by a lower-than-normal contribution of *C. finmarchicus* among the ten most abundant copepod species (Fig. 20c). At Shediac Valley station, the observed total copepod abundance in 2013 was well below the long-term average, with the maximum *C. finmarchicus* contribution observed in September and October, i.e., two months later than the long-term average (Fig. 20d–f).

In 2013, the abundance of *C. finmarchicus* was well below the long-term average, particularly from June to late August. This period was followed by an abrupt increase in abundance closer to normal in fall (Fig. 21a). The peak contribution of early stages was centred in August, which was much later than the 2005–2010 average centred in June, and coincided with the period of very low population abundance (Fig. 21a–c). Stage CV dominated the fall population despite the low summer abundance (Fig. 21c), suggesting that the downstream transport of local production to the wGSL and its recirculation into the Estuary was probably a dominant feature of the 2013 dynamics (Maps et al. 2011). At Shediac Valley station, the upstream supply of young *C. finmarchicus* stages from the Gaspé Current is shorter in time compared to the long-term average but with another peak in August (Fig. 21f). Once again, this pattern must be interpreted with caution since there was only one observation per month in 2013.

The abundance of the large-bodied *C. hyperboreus* was near (April–Aug.) or above (Sept.–Nov.) the long-term average at Rimouski station in 2013 and mostly below average at Shediac Valley station, most notably in June and July (Fig. 22a, d). While the relative CI–III copepodite abundance pattern was similar to the long-term climatology at Shediac Valley station (although we do not see the peak in early stages, which might have been missed because sampling started only in May), these early stages were nearly absent in samples from Rimouski station in 2013 (Fig. 22c, f).

The abundance of *Pseudocalanus* spp. at Rimouski station was mostly slightly below or near normal in 2013 (Fig. 23a). Population stage composition averaged from 2005 to 2010 showed that early stages were observed throughout the year (potential for several generations) (Fig. 23b). However, there were large peaks in the relative abundances of stage CII in May and CI–III in July in 2013 (Fig. 23c). No stage analysis was carried out for this species at Shediac Valley station.

Gulf subregions

The averaged total zooplankton biomass values for the GSL subregions during the spring and fall 2013 surveys were within the range of values seen throughout the time series (Fig. 24). The total zooplankton biomass in 2013 was similar to 2012 in the wGSL and eGSL but lower in the sGSL. In general, the total zooplankton biomass in the sGSL in spring shows greater interannual variability than in the other GSL regions and has been much higher than in fall for some years, although this difference was attenuated in 2013. These marked differences in zooplankton biomass among years in the sGSL during the early part of the productive season have been previously ascribed to interannual differences in the influx of large-bodied *Calanus* spp. from deeper adjacent regions (Plourde et al. 2014). However, this pattern could also be caused by interannual variations in the spatial distribution of zooplankton biomass in the sGSL in June (de Lafontaine 1994), implying that samples taken on the TIDM section would not be always representative of the overall zooplankton population among years in this region.

Overall, the 2013 annual abundances of key copepod species in the three regions are consistent with patterns observed over the times series (Fig. 25, 26, 27). The exception is the fall abundance of *Pseudocalanus* spp. in the sGSL, which is the highest fall abundance in this time series (Fig. 27). Some of these indices appear to be quite stable in different parts of the study area (e.g., *C. finmarchicus* in the wGSL since 2008) while others vary greatly on different time scales, particularly in spring (e.g., *C. finmarchicus* and *C. hyperboreus* in sGSL in spring; *Pseudocalanus* spp. in eGSL and wGSL). A close examination of the stage structure of *C. finmarchicus* (not shown) indicates that the large interannual variations in this species' abundance during spring surveys were mainly caused by variations in CI–III abundance. These variations in early stage abundance could be caused by interannual variations in overall population productivity, in the relative timing of the spring surveys and *C. finmarchicus*

population development (phenology), or both. During fall surveys, interannual variations in population abundance were mainly caused by fluctuations in the abundances of overwintering stages.

Copepod phenology

We present a detailed figure showing the seasonal cycle of the relative proportions of *C. finmarchicus* copepodite stages at Rimouski station from 1994 to 2013 in order to provide an assessment of potential changes in zooplankton phenology in the GSL (Fig. 28). We used proportions to minimize any distortion caused by large interannual variations in absolute abundance. The comprehensive examination of this data set revealed notable changes in the developmental timing of this key copepod species. For example, the period of maximum contribution of stages CI–III (equivalent to their abundance maximum) shifted from mid- to late July during the 1994–2000 period to predominantly mid-June to early July in 2006–2012, and made a sudden shift to late summer in 2013 (Fig. 28). This trend toward earlier development in summer stages was also observed in CV until 2012, and this stage also showed evidence of later-summer increases in 2013. The long-term change in the timing of maximum occurrence that we observed for stage CVI (both sexes)—with an earlier timing from 2008–2012 relative to 1994–2005—shows some indication of shifting to later in the season in 2013, although this is not so striking as it is for the early stages. The late occurrence of early stage (CI–CIII) abundance in the region could be associated with an abnormally high freshet from the St. Lawrence River in June 2013 (Galbraith et al. 2014). Some time periods (e.g., 2004) seem to show no emergence of CI–CIII stages. This is an artifact caused by the smoothing method used (Loess), which reduces the magnitude of smaller values. Nevertheless, this graph represents general trends in *C. finmarchicus* phenology.

Scorecards

A synthesis of basic AZMP zooplankton indices (abundances of *C. finmarchicus*, *Pseudocalanus* spp., total copepods, non-copepods) was performed using annual standardized abundance anomalies and is presented as a scorecard (Fig. 29). The reference period used to standardize annual abundances with the whole time series ranges from 1999 (2005 for Rimouski station) to 2010. If very high abundances appear after this period, they will not be included in the reference period and thus will generate high anomalies and larger contrasts between pre- and post-2010 values. In general, these annual indices were relatively coherent through the time series at fixed stations and within the large subregions. After three years of strong negative abundance anomalies from 2009–2011, *C. finmarchicus* returned to near-normal values in 2012 but then went back to strongly negative anomalies in 2013. The smaller *Pseudocalanus* spp. showed the opposite pattern, with positive abundance anomalies in 2010–2011 in all regions, a decrease to negative anomalies in 2012, and a return to near-normal or positive values in 2013. Total copepod abundance was generally close to the long-term normal in 2011, but anomalies grew increasingly negative between 2012 and 2013. Finally, the strong positive anomalies in non-copepod abundance that were seen in 2011 (eGSL) and 2012 (at Shediac Valley station) have attenuated somewhat, although the anomaly at Rimouski station went from negative to strongly positive (by almost 4 SD) from 2012 to 2013. The strong anomalies observed for non-copepods were caused by high abundances of larvaceans (*Fritillaria* spp. and *Oikopleura* spp.), gastropods (*Limacina helicina* and *L. retroversa*), and polychaete larvae.

The annual standardized abundance anomalies for a set of zooplankton indices are presented in Figure 30. Again, these annual indices were relatively coherent among the fixed stations and large regions over the time series. *C. hyperboreus* abundance returned to near-normal values in

2013 after having had strongly positive anomalies in 2012; this coincided with the *C. finmarchicus* decrease between 2012 and 2013 (Fig. 29) and resulted in a lower-than-normal abundance of large calanoids in 2013 (Fig. 30). Lower-than-normal abundances of large calanoids have been the norm in the GSL since 2009 (except for in 2012). Small calanoid abundances remained mostly near the normal in 2013 except for Shediac Valley station, which was probably due to a single high value of *Pseudocalanus* spp. abundance that was eight times higher than all other observations made during the year (Fig. 23d). There were two striking results revealed by the 2013 scorecard. One was the strong negative anomalies over the whole region for cyclopoids (dominated by *Oithona* spp. and the poecilostomatoid *Triconia* spp.), which could have contributed to the negative total copepod anomaly observed in 2013 (Fig. 29, 30). The other was the strong positive anomalies for warm-water species (predominantly *M. lucens*) at Rimouski station and in the wGSL, although the strong positive anomalies caused by other warm-water species (*Centropages* spp., *Clausocalanus* spp., *Paracalanus* spp.) seen in 2012 in the sGSL and eGSL have returned to near-normal values (Fig. 30). Finally, the abundance of cold/arctic copepod species (*C. glacialis*, *M. longa*), which was above normal in several areas in 2012, showed consistently negative anomalies over the whole GSL in 2013 (Fig. 30). Note that these indices are based on generally rare taxa, implying that relatively minor changes in abundance could result in large variations in their anomalies.

DISCUSSION

In 2013, a set of physical indices, including surface and cold intermediate layer temperatures as well as ice season duration, indicated that temperature conditions have remained well above the normal after their peak in 2012 (Galbraith et al. 2014). In addition, deep-water temperature in the GSL continued its increase in 2013 to values seldom observed since the early 1980s (Galbraith et al. 2014). This document reports on the chemical and biological conditions in the GSL in the context of a warm period that began in 2010 (Galbraith et al. 2014).

Winter maximum surface nutrient inventories in 2013 were close to the 2001–2010 average in many areas of the Estuary and GSL, ending the period of strong negative anomalies that was evident in 2010–2012. Winter mixing is a critical process to bring nutrient-rich deep water to the surface. In the GSL, this winter convection is in part caused by buoyancy loss (cooling and reduced runoff), brine rejection associated with sea-ice formation, and wind-driven mixing prior to ice formation (Galbraith 2006). Even though the seasonal maximum sea-ice volume was below normal and late winter water temperature was above normal in 2013—as observed in recent years—the thickness of surface mixed layer returned to near normal (Galbraith et al. 2014), which improved the supply of start-up nutrients for primary producers in 2013 compared to the 2010–2012 period. In addition to vertical mixing, the upwelling at the head of Laurentian Channel and the transport of nutrients via the Gaspé Current may also have contributed to increasing winter nutrient inventories for the estuarine portion and freshwater-influenced subregions of the GSL. Finally, water intrusions from the Labrador Shelf into the GSL were below normal in 2013 (Galbraith et al. 2014). Typically, these waters, which enter the Gulf via Cabot Strait during winter and flow in part northward along the west coast of Newfoundland, are relatively poor in nutrients compared to those that have originated from the Estuary or were mixed from deeper waters within the Gulf (see Fig. 8; climatology).

In contrast to expectations, the remote sensing of ocean colour data as well as the spring nitrate inventories revealed that the magnitude of the spring phytoplankton blooms in many areas of the GSL in 2013 were below or close to normal, although phytoplankton growth was initiated earlier in many regions, as has been observed in recent years. Changes in the ice cover can influence primary production by its influence on the light conditions in the water column (Le Fouest et al. 2005), and changes in stratification can also have either positive or negative

effects on primary production depending on water column conditions (Ferland et al. 2011). The shorter-than-normal ice period and the early warming/stratification (Galbraith et al. 2014) have contributed to the markedly early spring blooms in recent years (Plourde et al. 2014). The fact that utilization of nutrients during the spring was overall below normal in 2013 suggests that phytoplankton growth was regularly interrupted by turbulent mixing in many regions of the GSL. This is consistent with the fact that near-surface water temperatures (as revealed by satellite imagery) were often below normal from early spring to early fall, especially in the northwest Gulf (Galbraith et al. 2014).

In the lower St. Lawrence Estuary, the situation is somewhat different: the timing of the bloom was markedly delayed in 2013. Spring bloom timing in this region is recognized to be largely influenced by both runoff intensity and freshwater-associated turbidity (Levasseur et al. 1984, Therriault and Levasseur 1985; Zakardjian et al. 2000, Le Fouest et al. 2010, Mei et al. 2010). The spring bloom typically starts just after the spring–summer runoff peak. The shorter residence times and weak light conditions during higher freshwater runoff periods are two possible explanations for the delay in phytoplankton growth in this region in early summer compared to early spring in the GSL. Although the annual average runoff of the St. Lawrence River in 2013 was near normal, the spring freshet was above normal and persisted much longer than usual, with peak runoff in May that was nearly as high in June (Galbraith et al. 2014). This can explain the well-below-normal chlorophyll concentrations during spring–summer 2013 in the St. Lawrence Estuary and adjacent regions (i.e., the northwestern part of the Gulf). The weak summer phytoplankton production in the Estuary and the above-normal runoff could have promoted the transport of nutrients toward the southern part of the Gulf, an area where unusually high chlorophyll concentrations were observed during summer (July 2013; Fig. 16).

A shift to a smaller-sized phytoplankton community has also been observed in recent years (since 2004) at Rimouski station. In addition, the relative abundance of dinoflagellates has tended to be predominantly higher than normal in recent years, although this phenomenon was less notable in 2013. The markedly delayed spring diatom bloom in the St. Lawrence Estuary in 2013 can explain the unusual predominance of flagellates in the system during summer. Warmer temperatures, as observed in fall 2013 (Galbraith et al. 2014), are also associated with a shift toward greater flagellate and dinoflagellate predominance (Levasseur et al. 1984, Li and Harrison 2008), with potential consequences on copepod recruitment and zooplankton composition as well as on the flow of energy in marine food webs.

In 2013, deep-water temperatures and salinities were reported to be overall well above normal in the Gulf due to inward advection from Cabot Strait, where temperature and salinity reached record highs in 2012 at 200 and 300 m (Galbraith et al. 2014). Associated with this water mass, we observed deep nutrient levels (300 m) that were well above normal (Fig. 11). This was clearly unexpected, since the above-normal temperature and salinity indicate that a higher proportion of Gulf Stream water was entering the GSL compared to Labrador Shelf water, and the Gulf Stream is known to have lower nutrient levels. Further investigation is clearly needed on this unusual phenomenon, since this appears to be a recurrent event over the last few years (Galbraith et al. 2014). The warming of bottom waters and their above-normal nutrient levels (which will eventually be upwelled at the head of the Laurentian Channel) may have impacts on acidification previously reported in the region (Mucci et al. 2011), with potential negative consequences on fisheries and aquaculture activities as well as on global productivity and biodiversity in the GSL.

The high freshwater runoff observed in the St. Lawrence Estuary also impacted the zooplankton community, most notably by a lower-than-normal abundance of *C. finmarchicus* in summer (Fig. 21a) and a delayed timing of recruitment of early *C. finmarchicus* stages centred in August (Fig. 21c). The contribution of CI–III to the population abundance of *C. hyperboreus* in spring

was also lower than normal (Fig. 22c). This effect of freshwater runoff was likely a combination of downstream transport of surface-dwelling stages and a delayed onset of the spring phytoplankton bloom (Fig. 4), both of which could affect local population growth and abundance (Plourde et al. 2001, Maps et al. 2011). The absence of a second cohort of *C. finmarchicus* CI–III in fall at Rimouski station indicates that transport from the wGSL was the likely mechanism explaining the sharp increase of stage CV in September (Fig. 21a–c) (Maps et al. 2011).

In 2013, deep-water temperatures and salinity averaged over the Gulf increased slightly to reach the highest value since 1980 (Galbraith et al. 2014). A warm anomaly that was first observed in Cabot Strait a few years ago has propagated northwestward into the Gulf (Galbraith et al. 2014). Combined with surface water temperatures that remained generally above normal, these conditions could have resulted in the near-normal (sGSL, eGSL) or well-above-normal (Rimouski station, wGSL) abundances of warm-water copepod species in 2013 (Fig. 30). High positive anomalies in warm-water copepod species in the sGSL and eGSL in 2012 were caused by *Centropages* spp. and *Paracalanus* spp. (and somewhat by *Clausocalanus* spp.), most likely in response to near-record warm surface conditions. In contrast, the strong positive anomalies in 2013 in the wGSL were solely due to the high abundance of *M. lucens*, a mid-water species that might benefit from a warmer and saltier deep-water layer as well as from warmer environmental conditions at the surface and in the CIL (cold intermediate layer). Given the westward propagation of the warmer and saltier deep-water layer, it will be interesting to see if this positive anomaly in warm-water copepod species (*M. lucens*) will persist in 2014 in the wGSL and at Rimouski station.

Contrary to 2012, when cold-water copepod species (*C. glacialis*, *M. longa*) showed positive abundance anomalies in the sGSL and eGSL despite record-high surface temperatures, 2013 was characterized by generally lower-than-normal abundances of cold-water species across the region (Fig. 30). This pattern could reflect the cumulative effect of persistent warmer-than-normal environmental conditions on the local productivity of these species or changes in their transport from adjacent source regions. In 2013, the surface (surface and CIL temperature, ice volume) and deep (temperatures at depths > 200 m) composite anomalies were well above the normal for respectively the fourth and second consecutive years (Galbraith et al. 2014), indicating that all habitats exploited by *C. glacialis* and *M. longa* during various parts of their life cycle were warmer than normal for more than their normal life span. Plourde et al. (2002) showed a much lower abundance of *M. longa* in the lower estuary in 1979–1980, a period characterized by warm conditions similar to those observed since 2010, than during the cold conditions in the 1990s (Plourde et al. 2013). In addition, the abundance of *C. glacialis* on the Newfoundland Shelf is generally declining, suggesting that transport to the GSL from external source regions might have also declined (P. Pepin, DFO/NAFC, pers. comm.). The abundance of cold-water copepod species on the Scotian Shelf—downstream from the GSL—was also very low in 2013 (Johnson et al. 2014).

In 2013, the proportion of CIV in the overwintering *C. hyperboreus* population at Rimouski station was not only much lower than the 2005–2010 average (Fig. 22), but also low relative to the 2011 and 2012 values (Plourde et al. 2014). Such a low percentage of stage CIV following two years of high contribution was previously observed in the 1990s (Plourde et al. 2003), suggesting that this feature might not be related to the warm environmental conditions prevailing in the region since 2010. It rather reflects variations in the productivity of this species in the GSL or in its coupling with more local environmental conditions in the Estuary. In 2013, the abundance of *C. hyperboreus* decreased to near-normal values relative to 2012, suggesting that the low abundance of CI–III in spring and depleted CIV abundance in the overwintering population observed at Rimouski station might reflect an overall lower recruitment of this species in the region (Fig. 22, 30).

In addition to the environmental conditions affecting the bottom-up processes described above, 2013 was also characterized by events that could have profoundly modified the predation pressure experienced by large-bodied zooplankton species and affected their overall abundance. For the first time since the start of groundfish surveys in the GSL in 1990, a massive recruitment of the local redfish stock (*Sebastes mentella*) was observed, with the occurrence of 10 cm individuals (1 or 2 years old) in abundances several orders of magnitude greater than the 1990–2012 average (Archambault et al. 2014). Multi-frequency acoustic data collected on various surveys in the GSL in 2013 indicated that the bulk of the biomass of this massive cohort was centred between 150 and 200 m of depth (I. McQuinn, DFO/IML, unpublished data), i.e., overlapping with the overwintering depth of *C. finmarchicus* and to some extent with *C. hyperboreus* (Plourde et al. 2001, 2003). Several redfish individuals were captured in plankton nets during krill–whale surveys, and the examination of their stomach content revealed the presence of late-development *Calanus* stages along with small individuals of other macrozooplankton taxa. A quantitative assessment of the biomass of this new redfish cohort as well as a comprehensive description of its diet would be needed to determine whether its occurrence could have contributed to the lower abundance of *Calanus* species observed in 2013 relative to 2012.

SUMMARY

This document reports on the chemical and biological (plankton) conditions in the GSL in 2013 in the context of a strong warming event initiated in 2010. Data from 2013 are compared to time-series observations.

- Winter maximum surface nutrient inventories were close to the 2002–2010 average in many areas of the Estuary and GSL, ending the period of strong negative anomalies that was clearly evident in 2010–2012. This is consistent with the fact that winter mixing returned close to the normal in 2013 despite the below-normal sea-ice volume.
- The timing of the spring bloom in the Estuary and northwestern Gulf in 2013 was markedly delayed due to the strong spring freshet of the St. Lawrence River, causing strong negative anomalies in chlorophyll inventories and diatom abundances during spring–summer in these regions.
- In regions less influenced by the spring freshet of the St. Lawrence River, a shift to earlier timing of the spring bloom was clearly evident in the increased frequency of strong negative anomalies since 2010, although this phenomenon was less notable in 2013. This is consistent with the fact that winter conditions were more severe in 2013 relative to the highly anomalous warm conditions observed since 2010.
- There is evidence of a shift to a smaller phytoplankton community at Rimouski station that began in 2004. Warmer temperatures, such as those observed in fall 2013, could have contributed to a greater flagellate predominance in the system.
- The strong spring freshet of the St. Lawrence River likely impacted the zooplankton community, notably by a lower-than-normal abundance of *C. finmarchicus* (and low contribution of early stages CI–III) in summer and delayed recruitment (until August) of its early stages. The contribution of *C. hyperboreus* CI–III to the population abundance in spring was also lower than normal.
- The high Gulf-wide temperatures and salinities observed in 2013 could have resulted in above-normal abundances of warm-water copepod species at Rimouski station and in the wGSL. The strong positive anomalies in 2013 here were solely due to the high abundance of *M. lucens*, a mid-water species that might benefit from a warmer and saltier deep-water

layer as well as from warmer environmental conditions at the surface and in the cold intermediate layer.

- Contrary to the positive 2012 abundance anomalies of cold-water species (*C. glacialis*, *M. longa*) observed in the sGSL and eGSL despite record-high surface temperatures, 2013 was characterized by generally lower-than-normal abundances across the region. This pattern could reflect the cumulative effect of persistent warmer-than-normal environmental conditions on the local productivity of these species—all habitats exploited by *C. glacialis* and *M. longa* during various parts of their life cycle were warmer than normal for more than their life span—or changes in their transport from adjacent source regions, e.g., the Newfoundland Shelf.
- Historical evidence indicates that the low proportion of overwintering *C. hyperboreus* CIV might not be related to warm conditions but rather reflects production variability or its coupling to more local environmental conditions in the Estuary.
- In combination with the effects of environmental conditions, a strong cohort of 1- to 2-year-old *S. mentella* may have put strong predation pressure on large-bodied zooplankton and affected their overall abundance.

ACKNOWLEDGEMENTS

We thank Jean-Yves Couture and Sylvie Lessard as well as Isabelle St-Pierre and Caroline Lafleur for preparation and standardization of the phytoplankton and zooplankton data, respectively. The data used in this report would not be available without the work of François Villeneuve and his team (Sylvain Chartrand, Rémi Desmarais, Marie-Lyne Dubé, Yves Gagnon, Line McLaughlin, Roger Pigeon, Daniel Thibault, and the late Sylvain Cantin) for organizing and carrying out AZMP cruises and analyzing samples. Marie-France Beaulieu performed all zooplankton sample analyses. We thank Jeff Spry for providing data from the Shediac Valley station and BIO's remote sensing unit for the composite satellite images.

REFERENCES

- Archambault, D., H. Bourdages, C. Brassard, P. Galbraith, J. Gauthier, F. Grégoire, J. Lambert, and C. Nozeres. 2014. [Preliminary results from the groundfish and shrimp multidisciplinary survey in August 2013 in the Estuary and northern Gulf of St. Lawrence](#). DFO Can. Sci. Advis. Sec. Res. Doc. 2014/010 v + 97 pp.
- AZMP. 2006. [Physical and biological status of the environment](#). *AZMP Bulletin PMZA* 5: 3-8.
- Brickman, D., and B. Petrie. 2003. [Nitrate, silicate and phosphate atlas for the Gulf of St. Lawrence](#). Can. Tech. Rep. Hydrogr. Ocean Sci. 231: xi + 152 pp.
- de Lafontaine, Y. 1994. Zooplankton biomass in the southern Gulf of St. Lawrence: Spatial patterns and the influence of freshwater runoff. *Can. J. Fish. Aquat. Sci.*, 51(3): 617–635.
- DFO. 2013. [Oceanographic conditions in the Atlantic zone in 2012](#). DFO Can. Sci. Advis. Sec. Sci. Advis. Rep. 2013/057.
- Ferland, J., M. Gosselin, and M. Starr. 2011. Environmental control of summer primary production in the Hudson Bay system: The role of stratification. *J. Mar. Syst.* 88(3): 385–400.
- Galbraith, P. S. 2006. Winter water masses in the Gulf of St. Lawrence. *J. Geophys. Res.*, 111, C06022, doi:10.1029/2005JC003159.

-
- Galbraith, P. S., R. Desmarais, R. Pigeon, and S. Cantin. 2006. [Ten years of monitoring winter water masses in the Gulf of St. Lawrence by helicopter](#). AZMP Bulletin PMZA 5: 32–35.
- Galbraith, P. S., J. Chassé, P. Larouche, D. Gilbert, D. Brickman, B. Pettigrew, L. Devine, and C. Lafleur. 2013. [Physical oceanographic conditions in the Gulf of St. Lawrence in 2012](#). DFO Can. Sci. Advis. Sec. Res. Doc. 2013/026: v + 90 pp.
- Galbraith, P. S., J. Chassé, D. Gilbert, P. Larouche, C. Caverhill, D. Lefavre, D. Brickman, B. Pettigrew, L. Devine, and C. Lafleur. 2014. [Physical oceanographic conditions in the Gulf of St. Lawrence in 2013](#). DFO Can. Sci. Advis. Sec. Res. Doc. 2014/062: vi + 84 pp.
- Johnson, C., W. Li, E. Head, B. Casault, and J. Spry. 2014. [Optical, chemical, and biological oceanographic conditions on the Scotian Shelf and in the eastern Gulf of Maine in 2013](#). DFO Can. Sci. Advis. Sec. Res. Doc. 2014/104 v + 49 pp.
- Koutitonsky, V. G., and G. L. Bugden. 1991. The physical oceanography of the Gulf of St. Lawrence: a review with emphasis on the synoptic variability of the motion. In: J.-C. Therriault (ed.) The Gulf of St. Lawrence: small ocean or big estuary? Can. Spec. Publ. Fish. Aquat. Sci. 113: 57–90.
- Le Fouest, V., B. Zakardjian, F. Saucier, and M. Starr. 2005. Seasonal versus synoptic variability in planktonic production in a high-latitude marginal sea: the Gulf of St. Lawrence (Canada). J. Geophys. Res. 110, C09012, doi 10.1029/2004JC002423.
- Le Fouest, V., B. Zakardjian, and F. J. Saucier. 2010. Plankton ecosystem response to freshwater-associated bulk turbidity in the subarctic Gulf of St. Lawrence (Canada): A modelling study. J. Mar. Syst. 81(1-2): 75–85.
- Levasseur, M., J.-C. Therriault, and L. Legendre 1984. Hierarchical control of phytoplankton succession by physical factors. Mar. Ecol. Prog. Ser. 19: 211–222.
- Li, W. K. W., and W. G. Harrison. 2008. Propagation of an atmospheric climate signal to phytoplankton in a small marine basin. Limnol. Oceanogr. 53(5): 1734–1745.
- Maps, F., B. Zakardjian, S. Plourde, F.J. Saucier. 2011. Modeling the interactions between the seasonal and diel migration behaviors of *Calanus finmarchicus* and the circulation in the Gulf of St. Lawrence (Canada). J. Mar. Syst., 88: 183–202.
- Mei, Z. P., F. Saucier, V. Le Fouest, B. Zakardjian, S. Sennville, H. Huixiang Xie, and M. Starr. 2010. Modeling the timing of spring phytoplankton bloom and biological production of the Gulf of St. Lawrence (Canada): Effects of colored dissolved organic matter and temperature. Cont. Shelf Res. 30: 2027–2042.
- Mitchell, M. R., G. Harrison, K. Pauley, A. Gagné, G. Maillet, and P. Strain. 2002. Atlantic Zonal Monitoring Program sampling protocol. Can. Tech. Rep. Hydrogr. Ocean Sci. 223, iv + 23 pp.
- Mucci, A., M. Starr, D. Gilbert, and B. Sundby. 2011. Acidification of lower St. Lawrence Estuary bottom waters. Atmos.-Ocean 49(3): 206–218.
- Plourde, S., P. Joly, J. A. Runge, B. Zakardjian, and J. J. Dodson. 2001. Life cycle of *Calanus finmarchicus* in the lower St. Lawrence Estuary: imprint of circulation and late phytoplankton bloom. Can. J. Fish. Aquat. Sci. 58: 647–658.
- Plourde, S., J. J. Dodson, J. A. Runge, and J.-C. Therriault. 2002. Spatial and temporal variations in copepod community structure in the lower St. Lawrence Estuary, Canada. Mar. Ecol. Prog. Ser. 230: 221–224.
-

-
- Plourde, S., P. Joly, J. A. Runge, J. Dodson, and B. Zakardjian. 2003. Life cycle of *Calanus hyperboreus* in the lower St. Lawrence Estuary: is it coupled to local environmental conditions? *Mar. Ecol. Prog. Ser.* 255: 219–233.
- Plourde, S., F. Maps, and P. Joly. 2009. Mortality and survival in early stages control recruitment in *Calanus finmarchicus*. *J. Plankton Res.* 31(4): 371–388.
- Plourde, S., P. Galbraith, V. Lesage, F. Grégoire, H. Bourdage, J.-F. Gosselin, I. McQuinn, and M. Scarratt. 2013. [Ecosystem perspective on changes and anomalies in the Gulf of St. Lawrence: a context in support of the management of the St. Lawrence beluga whale population](#). DFO Can. Sci. Advis. Sec. Res. Doc. 2013/129. v + 30 pp.
- Plourde, S., M. Starr, L. Devine, J.-F. St-Pierre, L. St-Amand, P. Joly, and P. S. Galbraith. 2014. [Chemical and biological oceanographic conditions in the Estuary and Gulf of St. Lawrence during 2011 and 2012](#). DFO Can. Sci. Advis. Sec. Res. Doc. 2014/049. v + 46 pp.
- Therriault, J.-C., and M. Levasseur. 1985. Control of phytoplankton production in the Lower St. Lawrence Estuary: light and freshwater runoff. *Nat. Can.* 112: 77–96.
- Therriault, J.-C., B. Petrie, P. Pépin, J. Gagnon, D. Gregory, J. Helbig, A. Herman, D. Lefavre, M. Mitchell, B. Pelchat, J. Runge, and D. Sameoto. 1998. Proposal for a Northwest Atlantic zonal monitoring program. *Can. Tech. Rep. Hydrogr. Ocean Sci.*, 194: vii + 57 pp.
- Zakardjian, B. A., Y. Gratton, and A. F. Vézina. 2000. Late spring phytoplankton bloom in the Lower St. Lawrence Estuary: the flushing hypothesis revisited. *Mar. Ecol. Prog. Ser.* 192: 31–48.

TABLE

Table 1. List of AZMP missions with locations, dates, and sampling activities for 2013. wGSL, eGSL, and sGSL denote the western, eastern, and southern subregions of the Gulf of St. Lawrence. See Figure 1 for station locations.

Sampling Group	Name	Location	Dates	Vessel	Hydro	Net
Fixed	Rimouski	48°40.0'N/068°35.0'W	09 APR – 03 DEC	Beluga II	26	24
	Shediac Valley	47°46.8'N/064°01.8'W	09 MAY – 06 NOV	Multiple	8	8
Total					34	32
Sections	TESL	wGSL	02–12 JUN	Teleost	7	7
Spring	TSI	wGSL	02–12 JUN	Teleost	6	6
	TASO	wGSL	02–12 JUN	Teleost	5	5
	TIDM	sGSL	02–12 JUN	Teleost	10	10
	TDC	eGSL	02–12 JUN	Teleost	6	6
	TCEN	eGSL	02–12 JUN	Teleost	5	5
	TBB	eGSL	02–12 JUN	Teleost	7	7
Total					46	46
Sections	TESL	wGSL	29 OCT – 12 NOV	Hudson	7	7
Fall	TSI	wGSL	29 OCT – 12 NOV	Hudson	6	6
	TASO	wGSL	29 OCT – 12 NOV	Hudson	5	5
	TIDM	sGSL	29 OCT – 12 NOV	Hudson	10	10
	TDC	eGSL	29 OCT – 12 NOV	Hudson	6	6
	TCEN	eGSL	29 OCT – 12 NOV	Hudson	5	5
	TBB	eGSL	29 OCT – 12 NOV	Hudson	7	7
Total					46	46

FIGURES

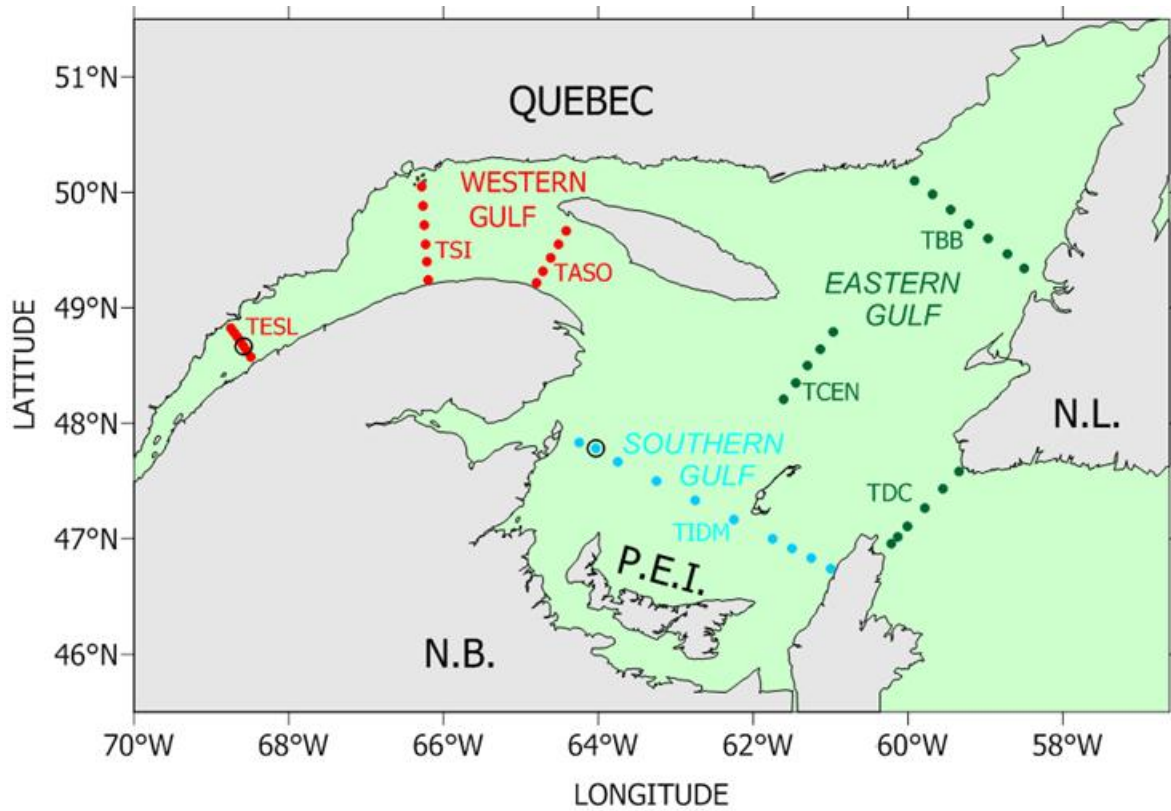


Figure 1. Map of the Estuary and Gulf of St. Lawrence showing sampling stations on the different sections (filled circles) and at fixed sites (open circles). GSL subregions are the western (red), southern (blue), and eastern (green) Gulf. Black circles show the locations for Rimouski station on the TESL line and Shediac Valley station on the TIDM line.

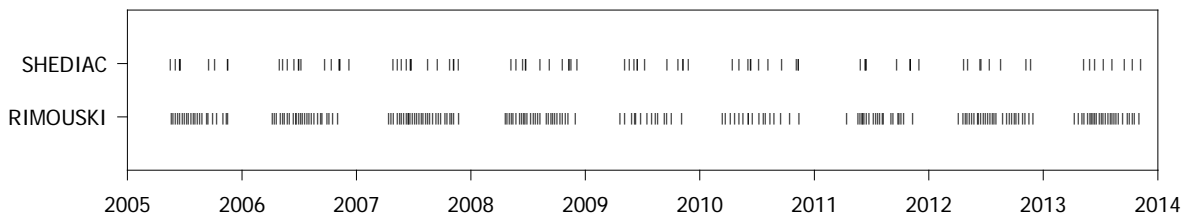


Figure 2. Sampling frequencies at Shediac Valley and Rimouski stations from 2005 to 2013 to show sampling effort in recent years.

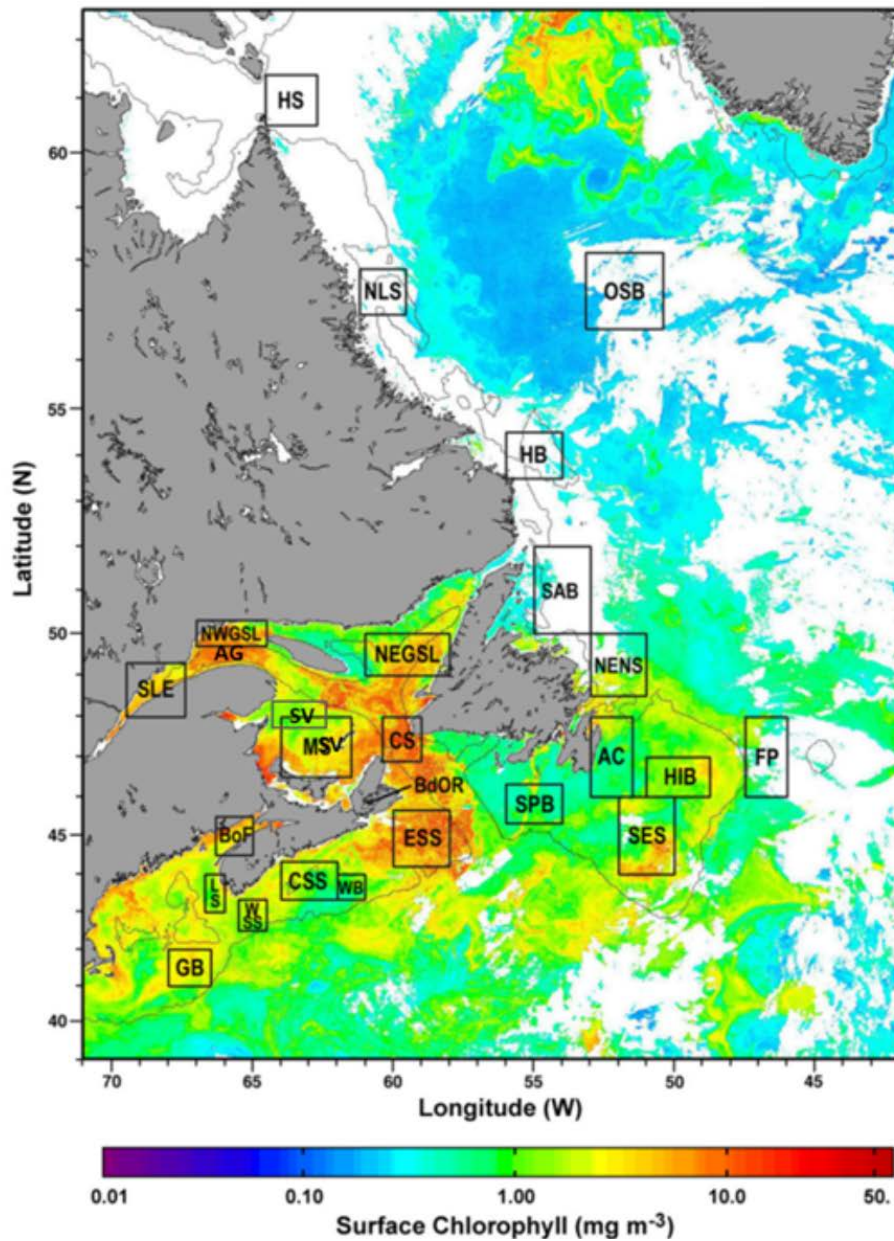


Figure 3. Statistical subregions in the Northwest Atlantic identified for spatial/temporal analysis of satellite ocean colour data. AC: Avalon Channel; **AG: Anticosti Gyre**; BdOR: Bras d'Or; BoF: Bay of Fundy; **CS: Cabot Strait**; CSS: Central Scotian Shelf; ESS: Eastern Scotian Shelf; FP: Flemish Pass; GB: Georges Bank; HB: Hamilton Bank; HIB: Hibernia; HS: Hudson Strait; LS: Lurcher Shoal; **MS: Magdalen Shallows**; **NEGSL: Northeast Gulf of St. Lawrence**; NENS: Northeast Newfoundland Shelf; NLS: Northern Labrador Shelf; **NWGSL: Northwest Gulf of St. Lawrence**; OSB: Ocean Station Bravo; SAB: St. Anthony Basin; SES: Southeast Shoal; SLE: St. Lawrence Estuary; SPB: St. Pierre Bank; **SV: Shediac Valley**; WB: Western Bank; WSS: Western Scotian Shelf. Only data from Gulf of St. Lawrence subregions (indicated in bold) are presented in this report. (The figure is a SeaWiFS composite image showing chlorophyll a from 1–15 April 1998.)

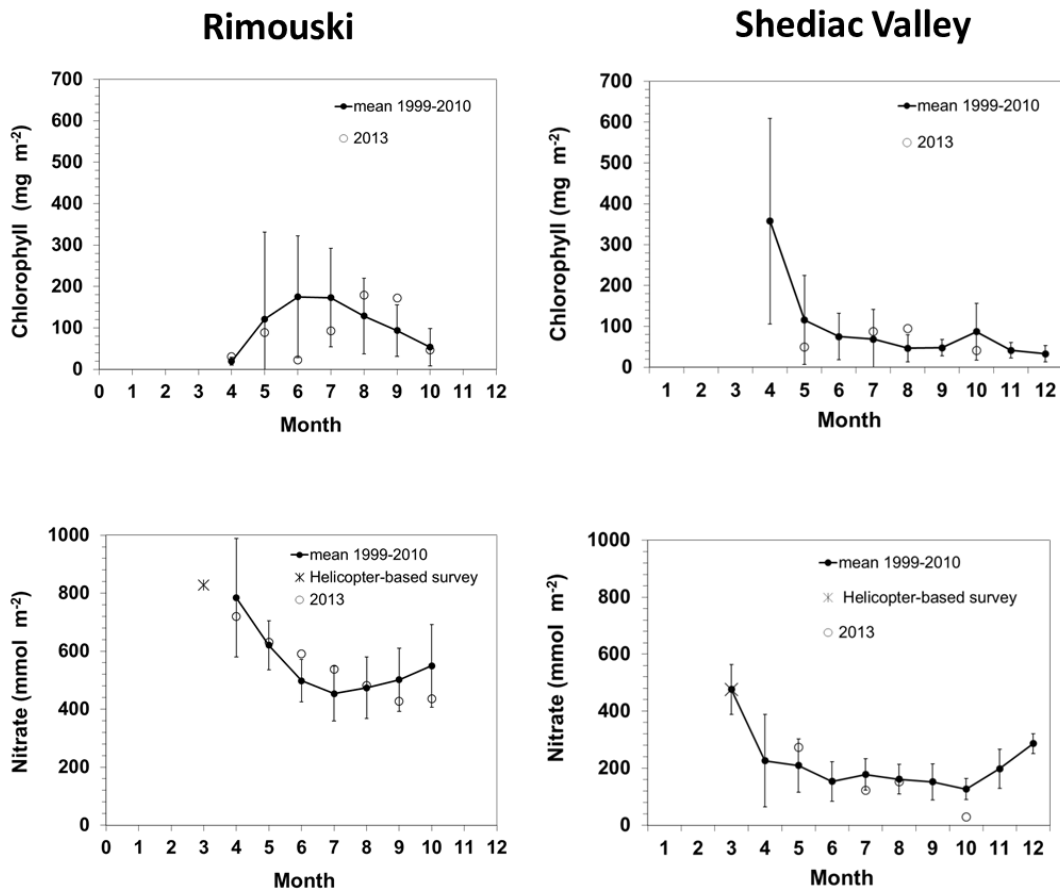


Figure 4. Chlorophyll (top panels; 0–100 m) and nitrate (bottom panels; 0–50 m) inventories in 2013 (open circles) with mean conditions from 1999–2010 (dots and solid line) at Rimouski and Shediac Valley stations. Vertical lines are the 95% confidence intervals of the monthly mean. Late winter nitrate values are from the March helicopter survey (samples from 2 m).

Station Rimouski

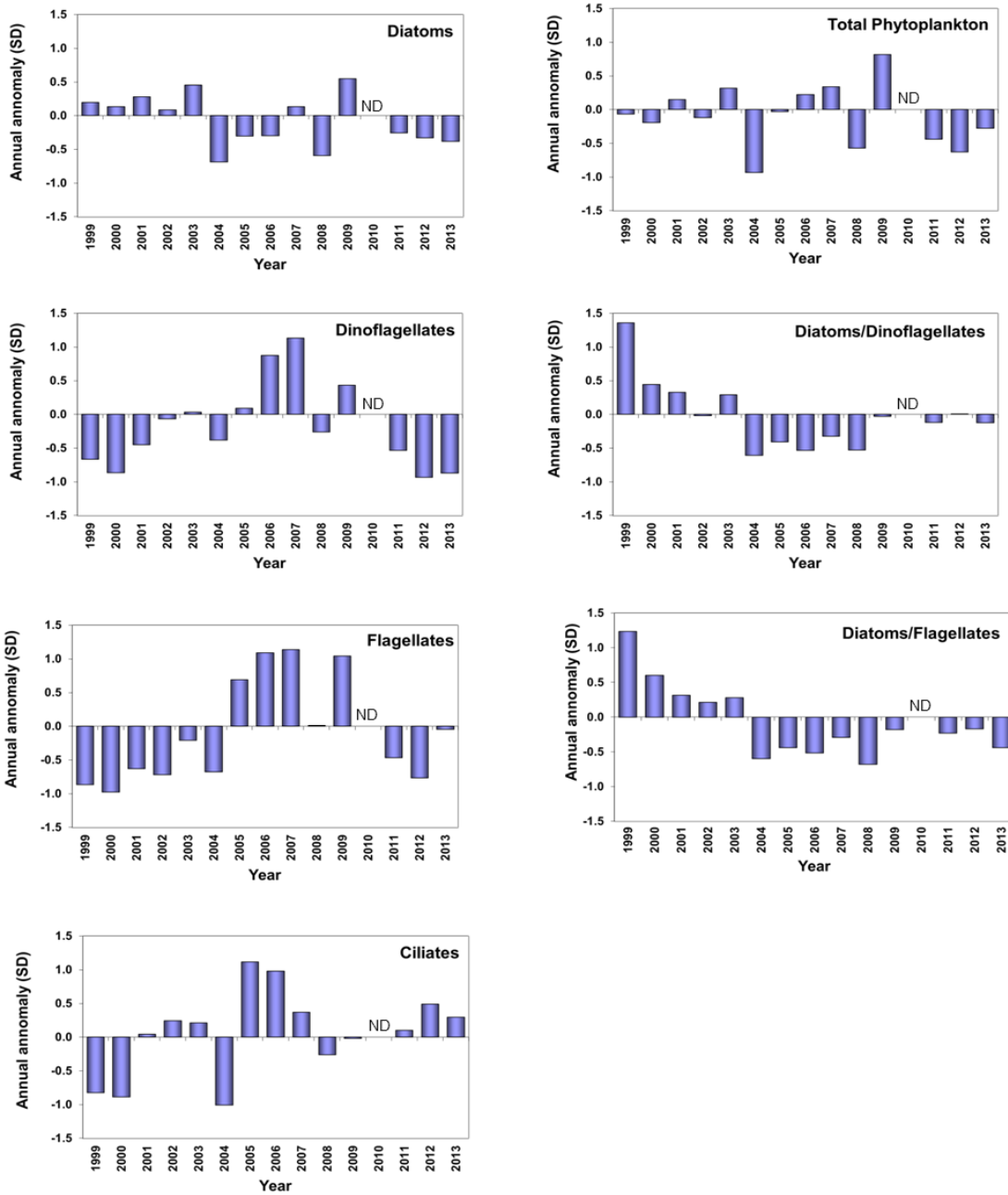


Figure 5. Time series of microplankton abundance anomalies for total phytoplankton and by group (diatoms, dinoflagellates, flagellates, ciliates), and for the diatom/dinoflagellate and diatom/flagellate ratios at Rimouski station, 1999–2013 (no data for 2010).

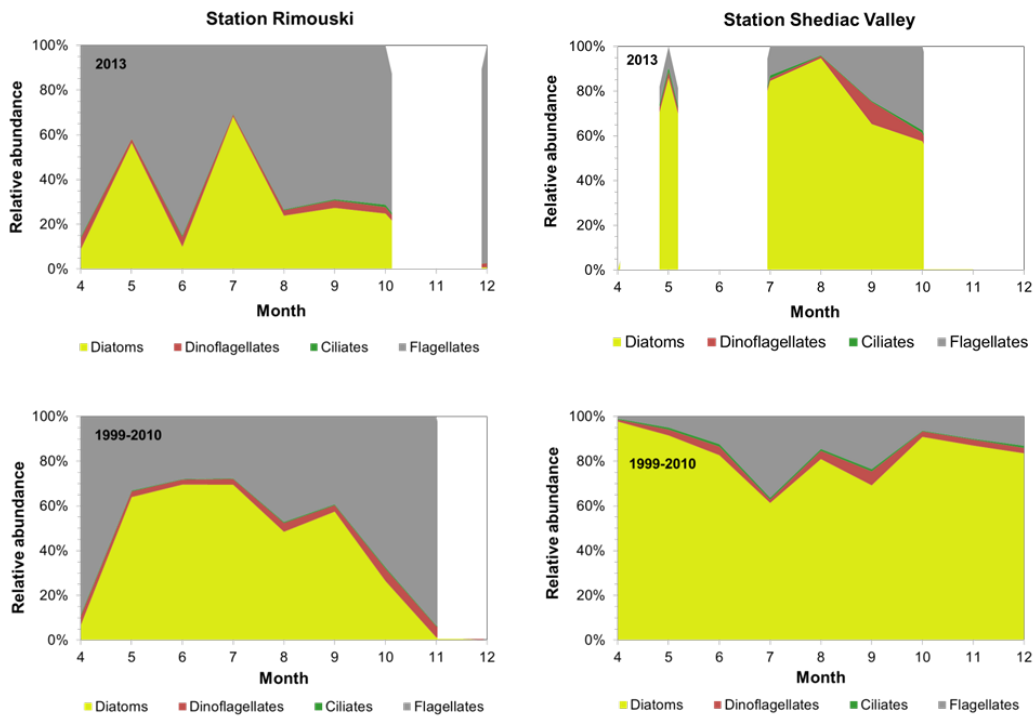


Figure 6. Phytoplankton community composition at Rimouski and Shediac Valley stations for 2013 (top panels) and for the 1999–2010 average (bottom panels). (The ciliate group is shown between the dinoflagellate and flagellate groups on the figures; it is usually so scarce that it is barely visible.)

Station Shediac Valley

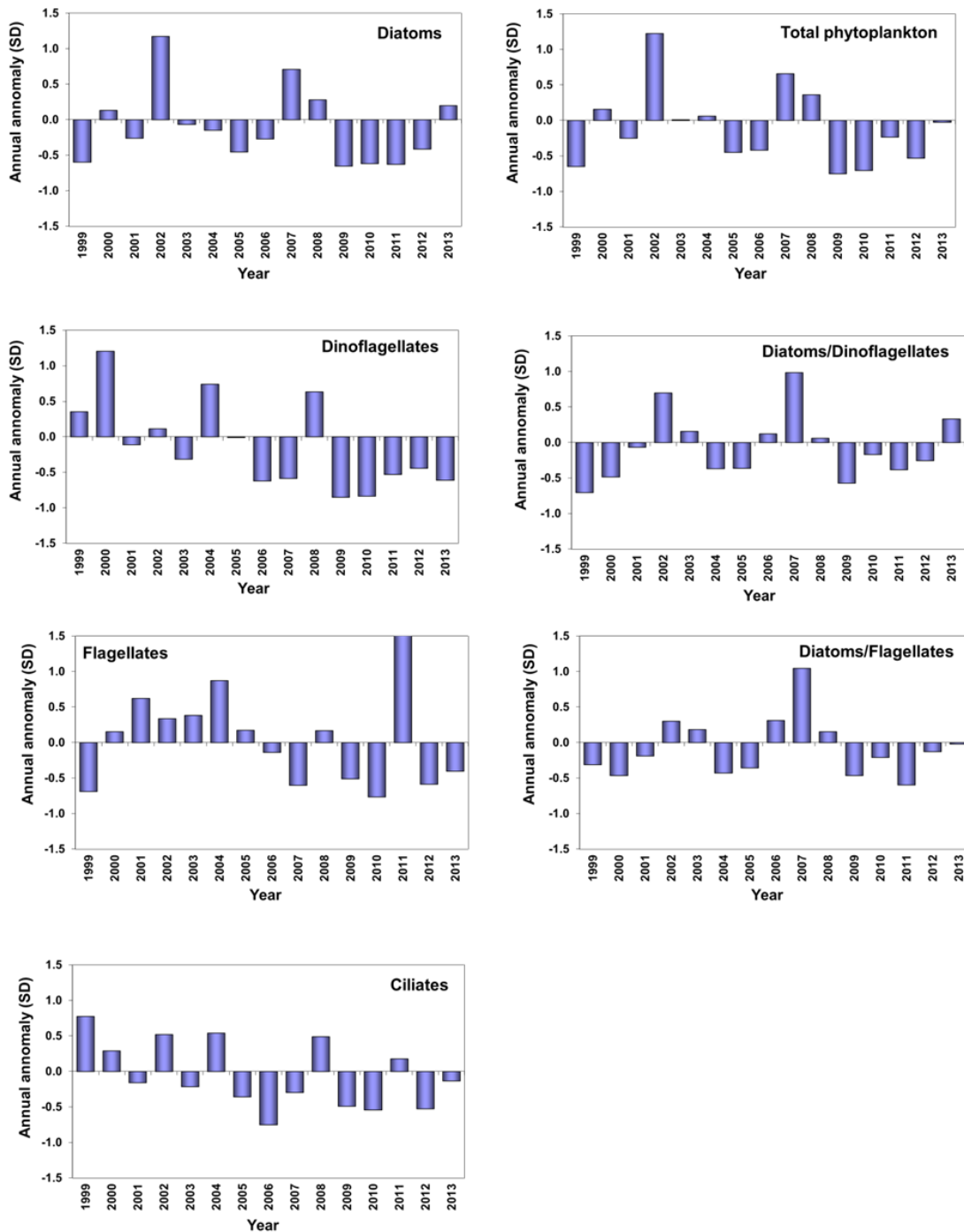


Figure 7. Time series of microplankton abundance anomalies for total phytoplankton and by group (diatoms, dinoflagellates, flagellates, ciliates), and for the diatom/dinoflagellate and diatom/flagellate ratios at Shediac Valley station, 1999–2013.

Nitrate

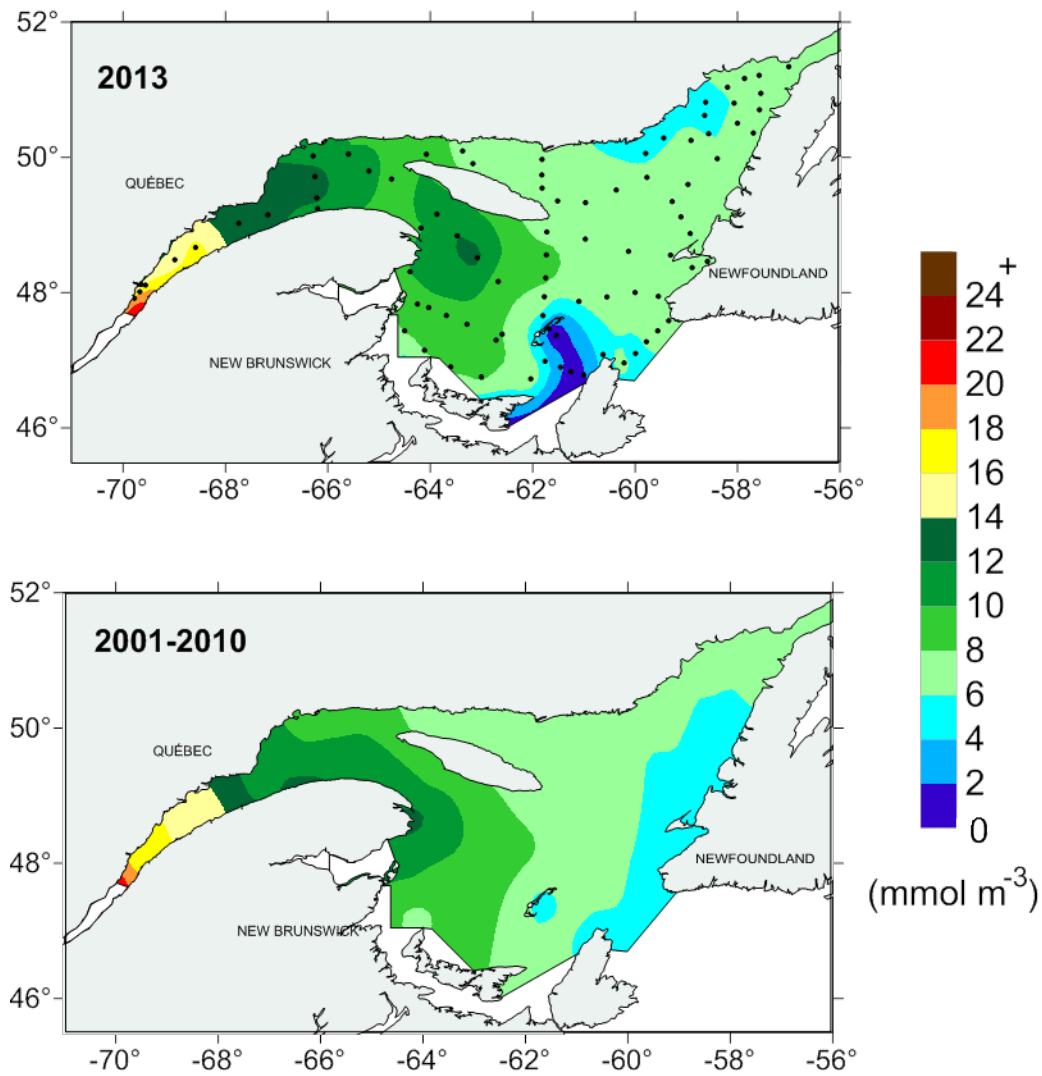


Figure 8. Concentrations of nitrate (mmol m^{-3}) at 2 m collected in the Estuary and Gulf of St. Lawrence during the helicopter survey in late winter (mid-March) 2013 compared to the 2001–2010 average. Dots indicate sampling locations.

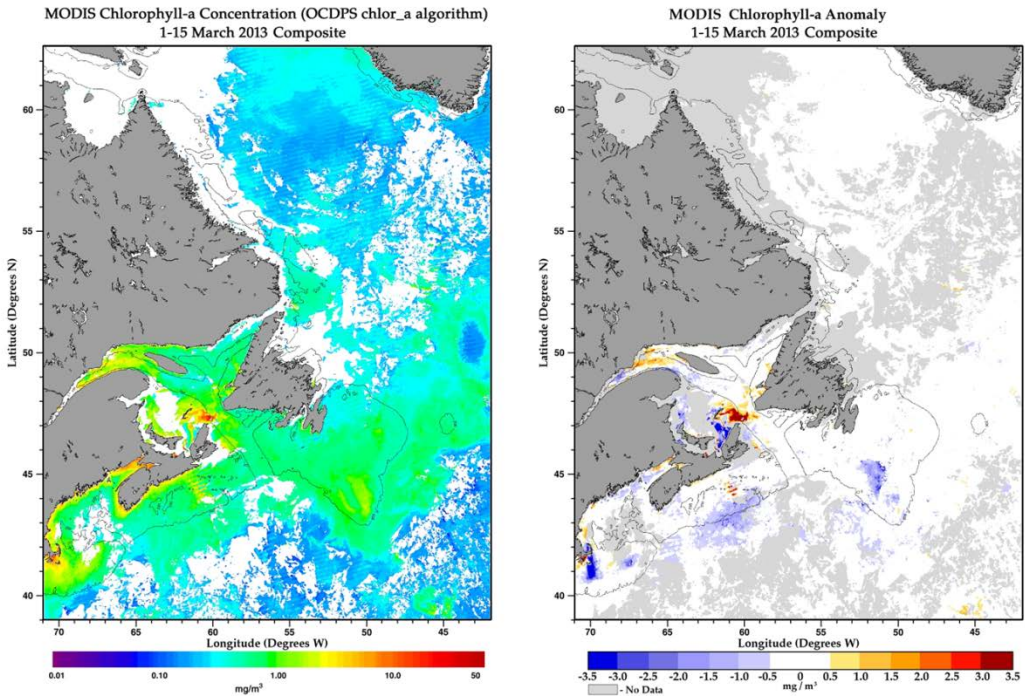


Figure 9. MODIS composite image of surface chlorophyll a (left) and chlorophyll a anomaly (right; based on the 2003–2010 reference period) in the Gulf of St. Lawrence. The images' date interval (1–15 March 2013) coincides with that of the late winter helicopter survey (5–14 March 2013).

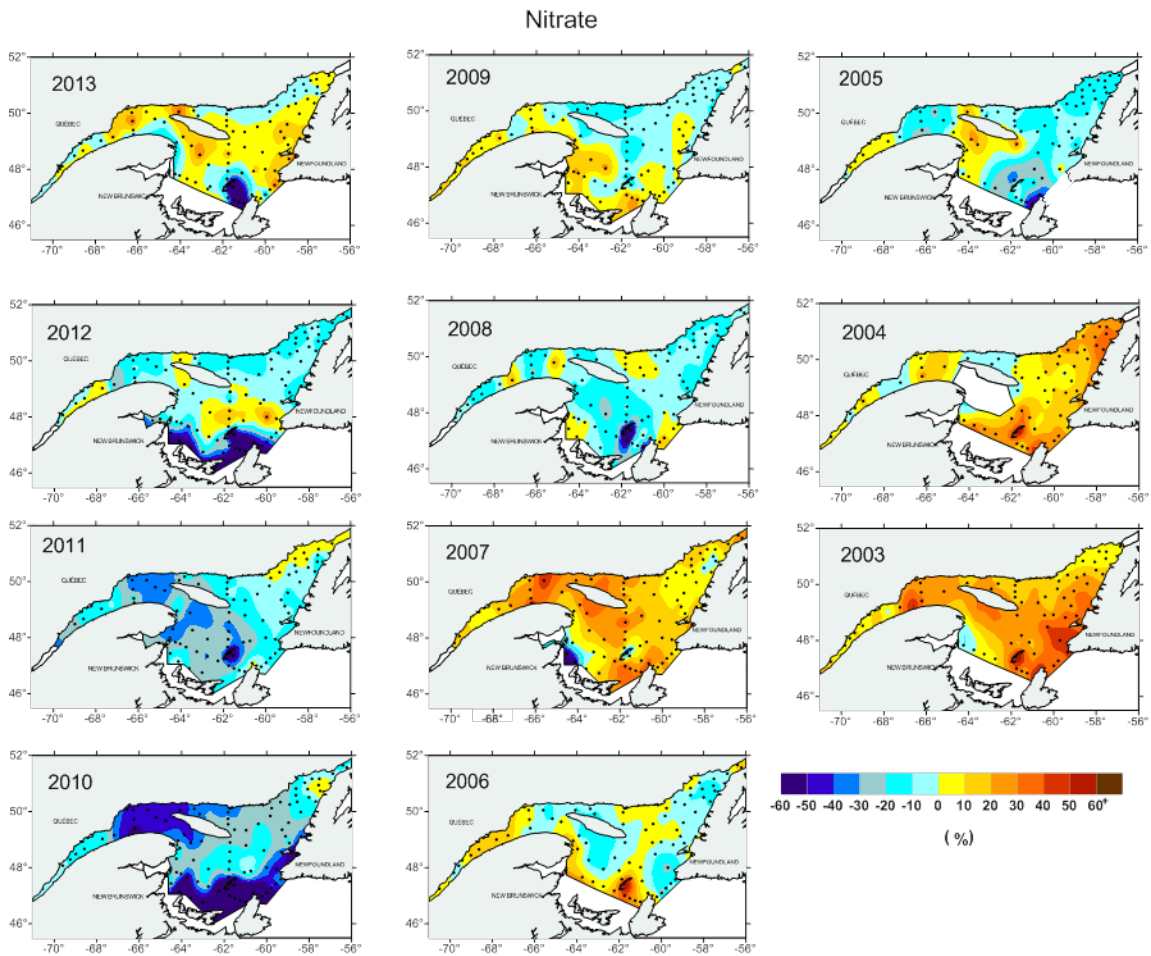


Figure 10. Percentage of change in the late winter (mid-March) nitrate concentrations at 2 m from samples collected during the helicopter survey from 2003 to 2013 relative to the 2001–2010 average. Dots indicate sampling locations.

Index	Transect	1999-2010												Mean	S.D.	%			
		1999	2000	2001	2002	2003	2004	2005	2006	2007	2008	2009	2010				2011	2012	2013
Winter nitrate inventory (0-50m) (mmol m ⁻²)	TESL			-0.33	-0.62	0.86	0.59		1.49	0.71	-1.51	0.19	-1.53	-1.72	-0.17	0.35	770	85	4
	TSI			-0.13	0.35	1.24	0.54	-0.76	0.02	1.26	-0.73	0.25	-2.06	-1.22	-0.43	0.35	528	125	13
	TASO			-0.23	0.05	1.21	-0.07	0.05	0.33	1.04	-0.15	0.25	-2.49	-1.85	-0.36	-0.44	522	89	-7
	TCEN			-0.65	-0.26	1.92	0.80	-0.94	-0.10	1.33	-0.62	-0.60	-0.89	-1.45	0.25	0.37	344	51	6
	TIDM			-0.02	0.44	0.58	0.91	-0.52	0.83	0.55	-0.76	0.38	-2.38	-0.93	-1.34	-0.84	384	99	-22
	TBB			-0.33	0.28	1.90	0.95	-0.72	-0.16	0.55	-0.70	-0.05	-1.72	-0.49	-0.63	0.52	299	38	7
	TDC			0.40	0.16	1.31	0.79	-0.98	-0.39	0.69	0.19	0.03	-2.20	-0.37	-1.02	0.15	293	80	4
Spring nitrate inventory (0-50m) (mmol m ⁻²)	TESL			0.01	1.67	-0.23	0.43		1.26	-0.79	-0.03	-0.95	-1.37	-0.58	0.23	1.61	437	92	34
	TSI	-1.21	-0.05	0.99	1.39	1.16	-0.70	-0.58	-0.02	-0.90	1.51	-0.59	-1.00	-1.04	-0.70	1.33	203	46	30
	TASO	-1.55	-0.62	-0.20	1.22	1.71	0.48	-0.67	-0.78	0.82	0.56	0.22	-1.20	-0.97	-1.26	1.46	186	59	47
	TCEN						-1.53	-0.01	0.96	-0.04	1.35	0.22	-0.95	-0.85	-1.62	2.55	68	20	74
	TIDM	-0.84	1.03	-0.83	-0.23	0.27	-0.62	-0.24	1.68	0.00	1.05	0.63	-1.91	-0.52	-0.99	0.89	109	38	31
	TBB	-0.33	0.34	-0.33	-0.30	2.50	-1.37	-0.96	-0.09	0.70	0.75	-0.59	-0.31	-1.13	-0.81	-1.30	63	24	-50
	TDC	-1.22	0.96	-0.24	-1.45	0.79	-0.12	-0.98	0.03	0.57	2.07	0.04	-0.45	-1.53	-0.69	-0.09	71	21	-3
Difference between winter and late spring nitrate inventory (0-50m) (mmol m ⁻²)	TESL			-0.25	1.86	0.87	0.11		0.12	1.22	-1.14	0.95	-0.03	-0.83	-0.31	-1.06	332	111	-35
	TSI			-0.44	-0.11	0.86	0.84	-0.50	0.10	1.63	-1.23	0.51	-1.64	-0.79	-0.13	0.10	319	126	4
	TASO			0.07	-0.84	0.29	-0.33	0.87	1.35	0.87	-0.51	0.33	-2.09	-1.43	0.85	-1.71	323	65	-35
	TCEN						1.45	-0.75	-0.30	1.41	-0.94	-0.51	-0.36	-0.93	0.97	-0.44	269	54	-9
	TIDM			0.35	0.61	0.55	1.34	-0.51	0.20	0.63	-1.38	0.15	-1.94	-0.86	-1.13	-1.40	275	84	-43
	TBB			-0.13	0.51	0.36	1.98	-0.13	-0.11	0.12	-1.28	0.36	-1.68	0.23	-0.14	1.47	236	35	22
	TDC			0.50	0.59	1.19	0.89	-0.77	-0.42	0.58	-0.37	0.03	-2.22	0.04	-0.89	0.20	221	75	7
Fall nitrate inventory (0-50m) (mmol m ⁻²)	TESL	2.49	-0.11	0.46	1.12	-0.61	-1.10	0.28	-0.78	-0.76	-0.07	-0.58	-0.33	-0.06	0.70	-0.45	534	116	-10
	TSI	1.91	-0.73	1.06	1.23	0.50	-1.28	-1.15	-0.32	-0.71	-0.49	-0.27	0.27	-0.46	1.57	0.71	268	102	27
	TASO	1.89	-0.29	0.86	1.19	-1.18	-1.04	-0.64	-0.34	-0.59	0.37	-1.03	0.81	-1.01	1.34	-0.01	278	74	0
	TCEN					-0.05	-0.91	-0.37	-0.25	2.09	0.17	0.47	-1.15	-2.83	-1.95	-1.10	136	28	-23
	TIDM		1.17	0.59	-0.04	-1.25	1.31	0.14	1.35	-0.93	-0.22	-0.91	-1.20	-2.15	-1.35	-0.19	183	36	-4
	TBB	0.94	0.33	1.27	0.12	0.79	-1.88	-0.29	-1.62	1.00	-0.38	0.24	-0.54	-0.51	-1.50	-0.97	125	31	-24
	TDC	1.44	0.73	-0.16	2.19	-0.59	-1.29	0.08	-0.11	-0.54	-0.61	-0.24	-0.91	-1.02	-0.50	0.12	135	45	4
Seasonally adjusted nitrate inventory (0-50m) (mmol m ⁻²)	TESL	2.60	0.09	0.02	0.97	-0.59	-0.58	0.47	-0.10	-0.88	-0.25	-0.85	-0.89	-0.46	0.21	0.19	511	120	5
	TSI	1.16	-0.64	1.27	1.56	0.86	-1.35	-1.20	-0.28	-0.94	0.16	-0.45	-0.15	-0.78	1.06	1.10	235	60	28
	TASO	0.66	-0.80	0.72	2.23	0.20	-0.67	-1.21	-1.00	0.07	0.84	-0.88	-0.15	-1.84	0.34	1.19	232	36	18
	TCEN					1.25	-1.42	-0.42	0.07	1.11	0.51	0.21	-1.31	-2.32	-2.10	0.24	106	23	5
	TIDM	-1.82	1.28	-0.02	-0.02	-0.37	0.46	0.07	1.72	-0.35	0.58	0.00	-1.52	-1.26	-1.10	0.51	142	36	13
	TBB	0.45	0.39	0.67	-0.08	1.82	-1.95	-0.69	-1.11	1.02	0.14	-0.14	-0.52	-0.92	-1.41	-1.32	94	23	-32
	TDC	1.03	1.37	-0.32	1.78	-0.26	-1.58	-0.43	-0.12	-0.32	0.41	-0.26	-1.31	-2.02	-0.96	0.09	103	19	2
Seasonally adjusted nitrate inventory (50-150m) (mmol m ⁻²)	TESL			1.04	1.56	0.18	-1.31		0.48	-0.04	-0.45	0.06	-1.52	-1.16	1.03	0.54	1336	110	4
	TSI	0.03	-1.39	0.73	1.24	0.95	-1.38	-0.87	0.68	-0.18	1.34	-1.07	-0.09	-0.50	1.09	0.61	1354	144	6
	TASO	-0.05	-1.53	0.20	1.36	0.89	-0.98	-1.00	1.01	-0.08	1.06	0.43	-1.31	-0.50	2.18	0.39	1256	100	3
	TCEN						-1.52	-0.28	1.19	0.69	0.31	0.68	-1.08	-0.91	-0.33	0.97	1093	106	9
	TIDM	-2.58	-0.17	-0.05	0.48	1.08	-1.03	-0.06	0.93	0.72	0.13	-0.12	0.67	0.42	0.40	0.60	898	99	7
	TBB	-1.07	1.90	-1.30	-0.01	0.27	-1.14	-0.62	1.51	-0.30	0.52	0.35	-0.10	-0.53	1.83	0.64	867	86	6
	TDC																		
Seasonally adjusted nitrate inventory (300m) (mmol m ⁻³)	TESL	2.49	-0.67	-0.35	0.14	-0.40	-0.20	0.48	0.77	-0.69	-0.04	-1.64	0.10	-0.56	0.24	0.31	23.9	1.5	2
	TSI	-2.20	-1.32	-0.16	0.84	1.07	-0.49	-0.36	1.19	0.48	0.70	0.19	0.05	0.40	1.52	2.58	23.5	0.8	9
	TASO	-0.52	-0.39	-2.17	0.52	-0.05	0.77	0.78	0.19	-1.55	0.84	0.82	0.76	-0.94	1.36	2.33	23.4	0.6	6
	TDC	-1.36	0.81	-0.18	-1.76	1.55	-0.13	-0.58	0.92	-0.32	0.12	-0.31	1.25	-1.96	1.42	1.92	21.9	0.4	7
Spring chlorophyll concentration (0-100m) (mg Chl m ⁻²)	TESL		0.00	0.97	-0.93	1.65	-0.91	0.00	-0.97	1.10	-0.66	-0.07	-0.19	-0.40	-0.10	-1.22	153	98	-80
	TSI	-0.18	-1.35	0.08	2.29	-0.34	1.32	0.22	0.21	-0.90	-0.66	0.08	-0.25	0.46	-1.23	69	38	-67	
	TASO	-0.43	-0.68	-0.73	2.79	-0.38	0.54	0.50	0.38	-0.71	-0.60	-0.56	-0.13	-0.55	-0.12	-0.98	94	67	-71
	TCEN						-0.84	-0.62	-0.74	0.63	1.73	0.62	-0.77	-0.84	-0.94	-0.02	38	12	-1
	TIDM	-0.20	-1.56	-0.51	2.41	0.27	-0.07	-0.72	-0.01	-0.21	-0.45	-0.21	1.25	-0.20	-0.25	0.56	35	14	22
	TBB	-0.96	0.47	-1.16	1.64	-0.81	1.74	-0.66	-0.84	-0.13	0.81	-0.46	0.35	-1.06	-0.43	1.61	30	10	58
	TDC	2.01	-0.62	-0.01	2.10	-0.68	-0.73	-0.74	-0.12	-0.45	-0.50	-0.36	0.08	-0.47	-0.41	-0.44	47	32	-30
Fall chlorophyll concentration (0-100m) (mg Chl m ⁻²)	TESL	-0.71	-1.63	-0.64	-0.12	0.20	0.18	-0.29	-0.07	0.02	2.41	-0.23	-0.12	-0.41	0.73	-0.96	23	9	-37
	TSI	-0.45	-0.86	-0.57	-0.19	0.26	0.41	-0.32	-0.24	2.98	-0.52	-0.25	-0.54	-0.29	-0.51	46	34	-37	
	TASO	-0.57	-0.95	-0.55	-0.17	0.64	-0.52	0.23	-0.12	-0.19	2.89	-0.14	-0.54	-0.27	0.11	-0.01	45	32	0
	TCEN					1.29	-1.41		-0.87	-0.57	0.20	0.31	1.06	-1.48	0.00	-0.20	42	8	-4
	TIDM		-1.64	0.59	1.71	0.79	-0.85	-0.85	-0.44	1.22	-0.50	-0.12	0.09	0.48	1.67	2.12	38	17	73
	TBB	-0.58	-1.36	-0.27	1.37	1.01	2.09	-0.60	-0.72	0.26	-0.59	-0.22	-0.38	0.99	0.78	0.40	35	11	12
	TDC	-0.91	-1.70	-0.24	1.53	0.35	-0.30	-0.82	0.79	1.07	-0.45	1.29	-0.61	-0.76	-0.66	1.11	41	11	30
Seasonally adjusted chlorophyll concentration (0-100m) (mmol m ⁻²)	TESL	-1.01	-1.16	1.16	-0.53	1.93	-0.49	-0.94	-0.56	1.33	-0.08	0.23	0.14	-0.08	0.28	-0.89	71	54	-68
	TSI	-0.49	-1.80	-0.36	1.80	-0.10	0.93	-0.38	-0.01	0.00	1.48	-0.96	-0.12	-0.62	0.17	-1.43	58	22	-55
	TASO	-0.66	-1.06	-0.93	2.55	-0.08	0.28	0.57	0.30	-0.75	0.73	-0.59	-0.36	-0.64	-0.06	-0.92	69	36	-48
	TCEN						-1.22	-1.04	-0.91	0.14	1.21	0.53	-0.05	-1.25	-0.65	-0.12	40	9	-3
	TIDM	-0.54	-1.48	-0.74	0.89	0.34	-0.24	0.05	-0.23	-0.39	2.52	-0.56	0.38	-0.57	-0.29	-0.15	37	16	-7
	TBB	-0.87	-0.54	-0.80	1.72	0.15	2.20	-0.72	-0.90	0.08	0.10	-0.38	-0.03	-0.03	0.21	1.15	32	9	33
	TDC	1.51	-1.08	-0.08	2.35	-0.49	-0.74	-0.92	0.14	-0.07	-0.59	0.08	-0.12	-0.66	-0.57	-0.05	44	18	-2

Figure 11. Normalized annual anomalies (scorecard) for nutrient inventories and chlorophyll levels at sections during the winter, late spring, and fall surveys. Blue colours indicate anomalies below the mean and reds are anomalies above the mean. Percentages of change in the 2013 values relative to the 1999–2010 average are shown to the right of the table.

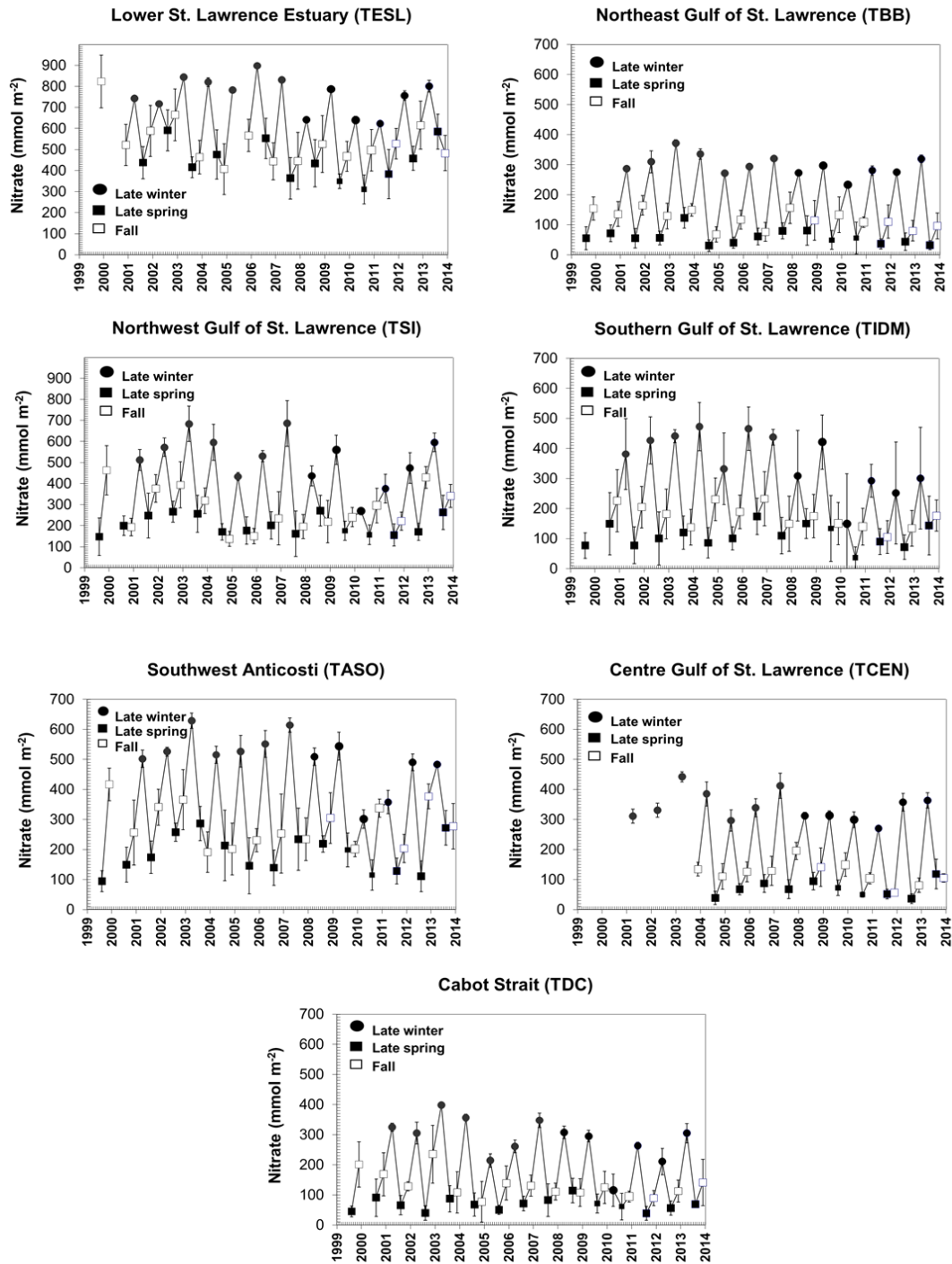


Figure 12. Time series of surface (0–50m) nitrate inventories along the seven AZMP sections from 1999 to 2013. The late winter inventories were calculated using surface (2 m) concentrations \times 50 m (assuming that the nitrate concentrations are homogeneous in the winter mixed layer at that time of the year). Note the different scale for the TESL and TSI graphs.

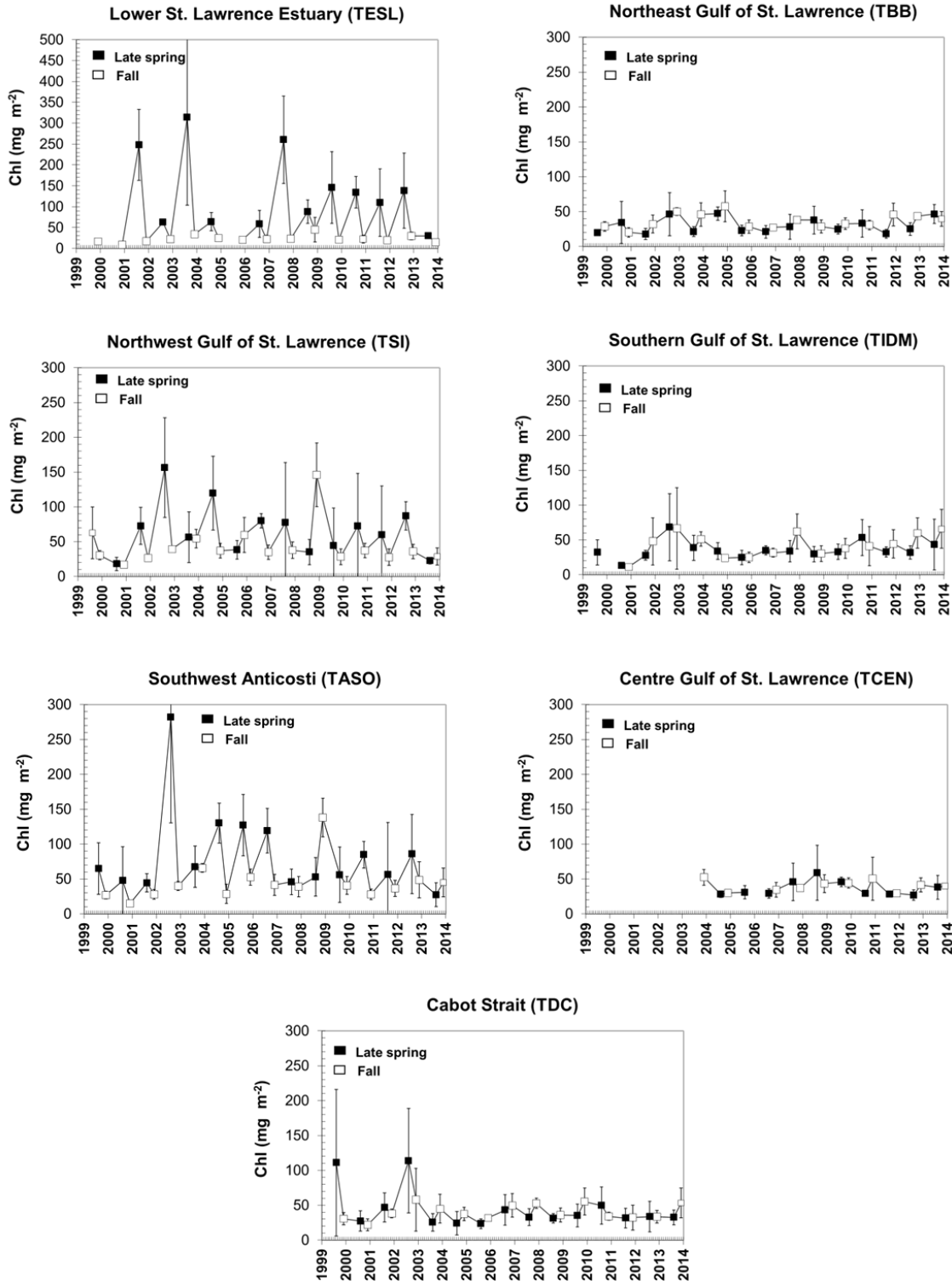


Figure 13. Time series of integrated (0–100 m) chlorophyll biomass along the seven AZMP sections from 1999 to 2013. Note the different scale for the TESL graph.

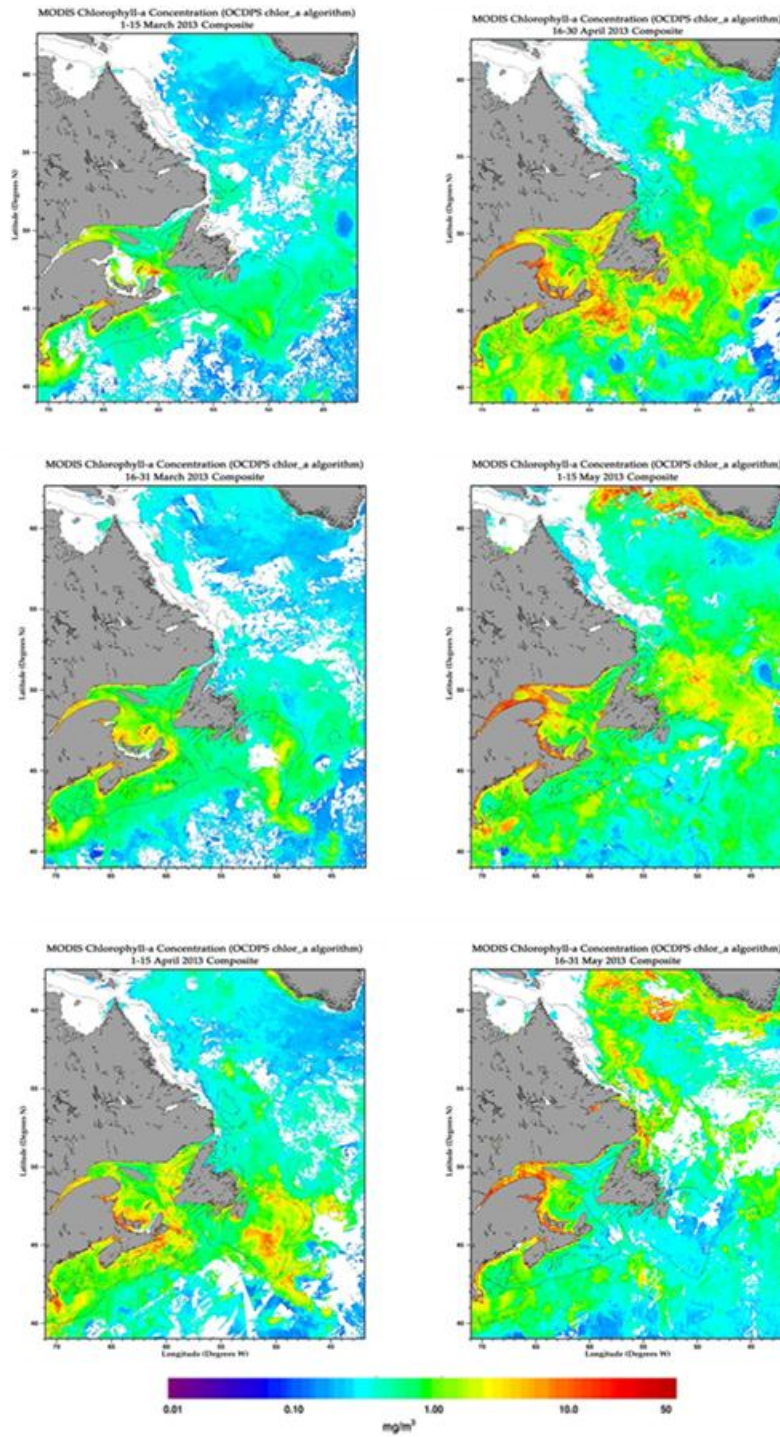


Figure 14. MODIS twice-monthly composite images of surface chlorophyll a in the Gulf of St. Lawrence during late winter – early spring (March–May) 2013.

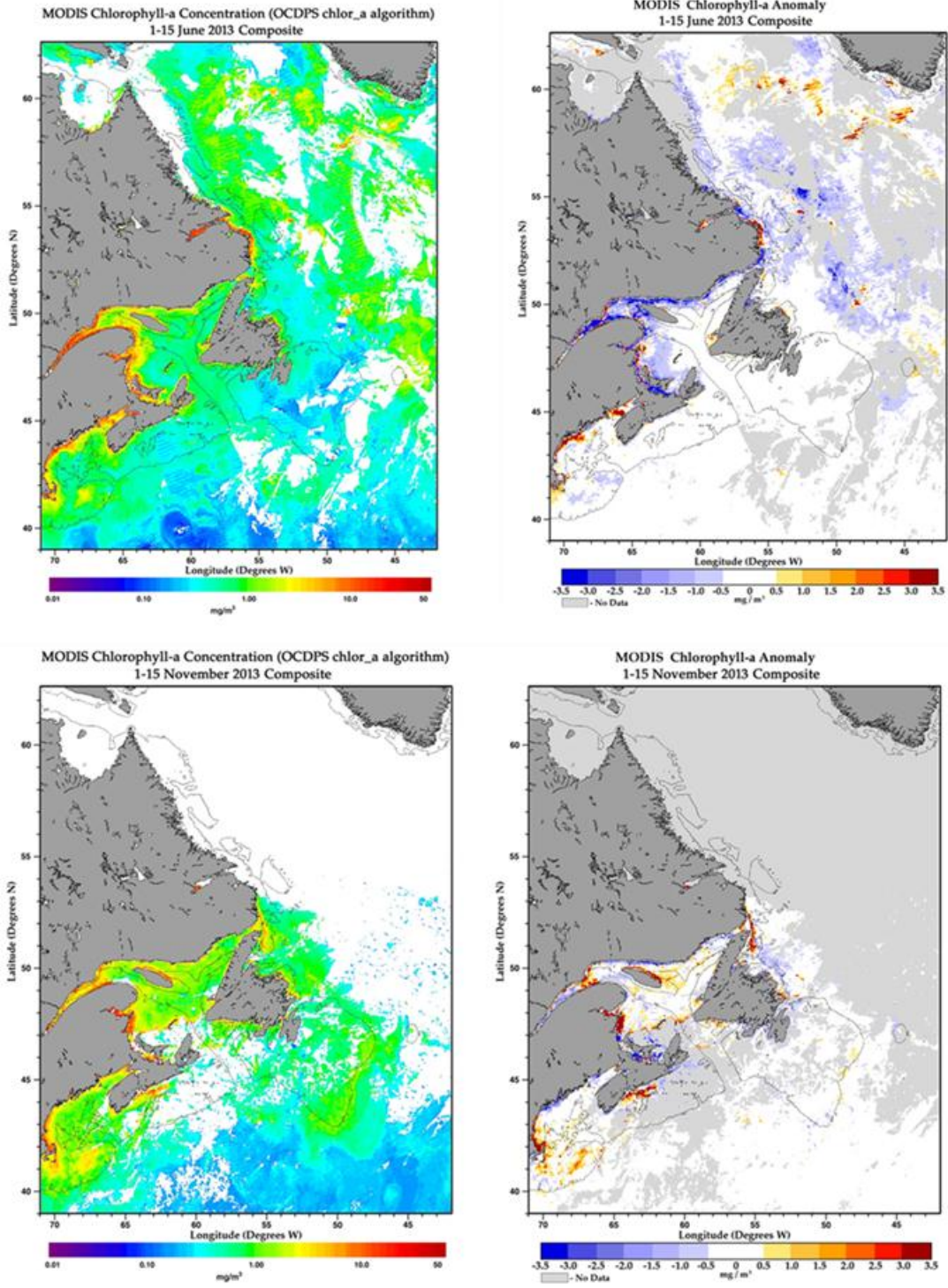


Figure 15. MODIS composite images of surface chlorophyll a (left) and chlorophyll a anomaly (right; based on the based on the 2003–2010 reference period) in the Gulf of St. Lawrence. The images' date intervals (1–15 June and 1–15 Nov. 2013) coincide with those of the late spring (2–12 June 2013) and fall (29 Oct. – 12 Nov. 2013) surveys.

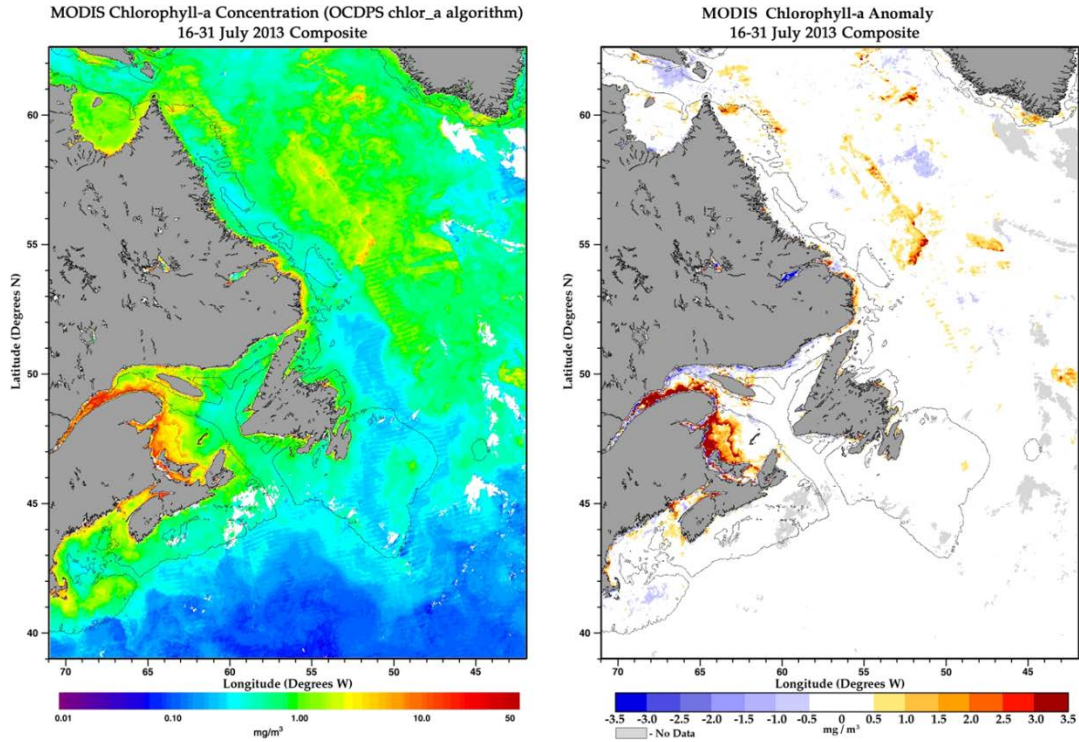


Figure 16. MODIS composite image of surface chlorophyll a (left) and chlorophyll a anomaly (right; based on the 2003–2010 reference period) in the Gulf of St. Lawrence showing the strong positive anomaly in late July 2013 in the St. Lawrence Estuary and the Southern Gulf (no concomitant field campaign).

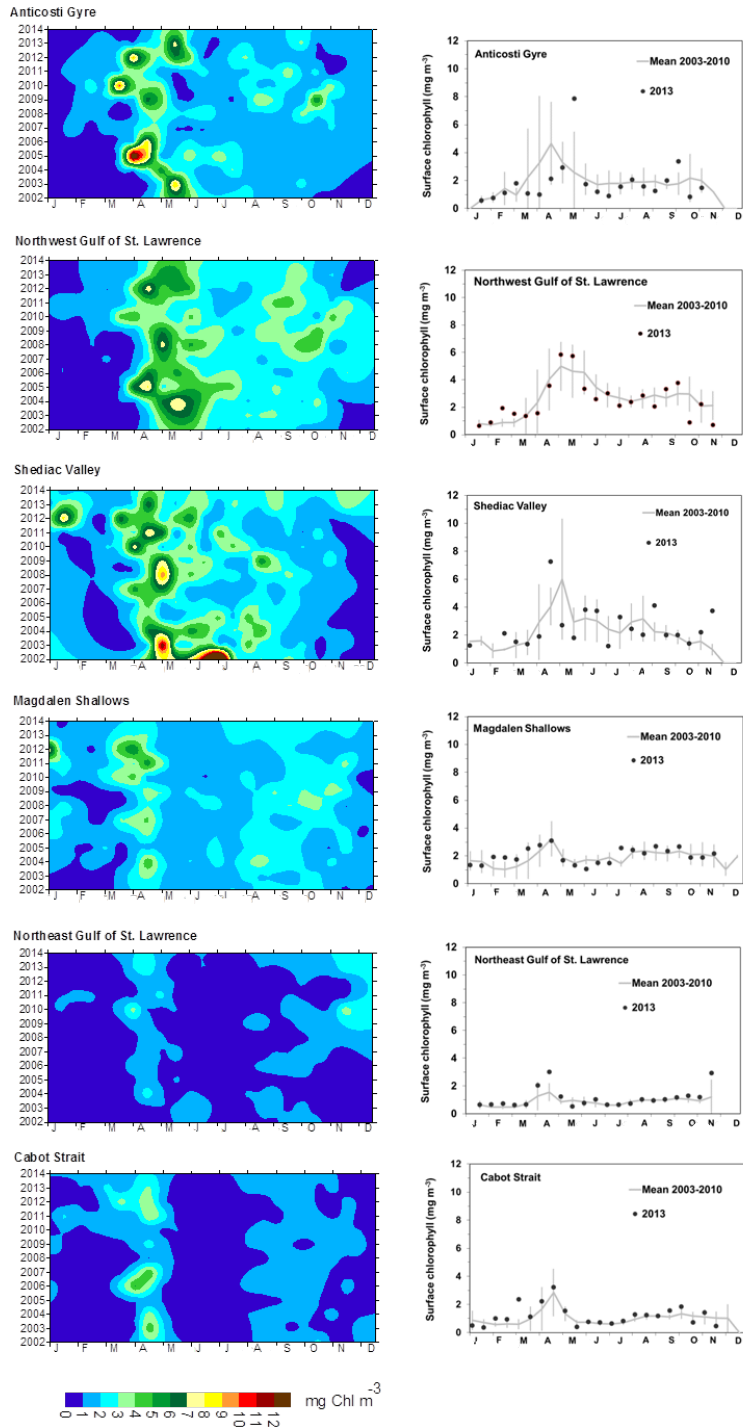


Figure 17. Left panels: Time series of surface chlorophyll *a* concentrations from twice-monthly MODIS ocean colour data in the Anticosti Gyre, Northwest Gulf of St. Lawrence, Shediac Valley, Magdalen Shallows, Northeast Gulf of St. Lawrence, and Cabot Strait statistical subregions (see Fig. 3). Right panels: comparison of 2013 (black circles) surface chlorophyll estimates from satellite ocean colour with mean conditions from 2003–2010 (solid line) for the same statistical subregions.

Indices of change in productivity based on MODIS twice-monthly ocean colour composites

Index	Subregion	2002	2003	2004	2005	2006	2007	2008	2009	2010	2011	2012	2013
Annual mean surface Chl (March to December)	Northwest Gulf of St. Lawrence		-0.69	0.24	1.24	-0.45	-1.82	1.15	0.30	0.03	-0.68	0.15	-0.82
	Anticosti Gyre		-0.51	-0.52	1.99	-0.49	-1.27	-0.25	0.38	0.68	-0.62	0.89	-0.42
	Shediac Valley		0.21	1.40	-1.07	-1.50	-0.53	1.04	0.34	0.41	-0.08	0.03	0.21
	Magdalen Shallows		-1.14	1.34	-1.19	-0.21	-0.01	-0.39	1.51	0.09	1.65	0.27	0.69
	Northeast Gulf of St. Lawrence		-0.40	0.14	-0.86	0.12	-0.14	-1.34	0.46	2.01	-0.59	-0.84	1.93
	Cabot Strait		-0.17	-0.32	-1.47	1.81	0.82	-0.84	-0.06	0.23	0.31	0.83	0.96
Spring bloom magnitude	Northwest Gulf of St. Lawrence		-0.39	1.16	1.34	-0.20	-1.16	0.88	-0.50	-1.14	-1.97	1.08	-0.69
	Anticosti Gyre		0.86	-0.36	0.60	0.54	-1.45	-1.33	-0.13	1.27	-1.35	0.77	0.27
	Shediac Valley		1.62	-0.20	-1.73	-0.72	-0.24	0.81	0.16	0.29	0.33	0.03	0.00
	Magdalen Shallows		-0.52	1.61	-1.50	-0.31	0.64	-0.77	-0.05	0.89	-0.15	2.73	-0.66
	Northeast Gulf of St. Lawrence		-0.49	0.89	-0.51	-0.25	-0.08	-0.89	-0.76	2.07	0.59	-0.70	1.30
	Cabot Strait		1.01	0.26	-1.19	1.18	1.05	-1.10	-0.40	-0.80	0.53	0.21	-0.06
Mean surface Chl - March to May	Northwest Gulf of St. Lawrence		-1.33	0.85	1.56	0.42	-1.20	-0.39	-0.34	0.44	-1.00	2.49	0.52
	Anticosti Gyre		-0.50	-0.37	2.09	-0.29	-0.93	-0.78	-0.06	0.84	-1.02	1.15	-0.19
	Shediac Valley		0.43	0.68	-1.55	-1.55	0.87	0.87	0.11	0.14	0.45	0.74	-0.75
	Magdalen Shallows		-0.36	0.35	-1.17	-0.28	1.33	-1.31	0.09	1.34	2.08	2.47	0.51
	Northeast Gulf of St. Lawrence		-1.25	0.61	-0.53	0.34	0.19	-0.83	-0.47	1.93	0.76	0.29	1.61
	Cabot Strait		0.24	-0.18	-1.07	1.79	1.01	-1.16	-0.33	-0.30	0.92	1.79	0.93
Mean surface Chl - June to August	Northwest Gulf of St. Lawrence		0.47	0.67	1.43	-0.16	-1.68	0.66	-0.58	-0.81	-1.63	-1.07	-0.75
	Anticosti Gyre		-0.05	-0.09	1.98	-0.05	-1.50	0.59	-0.21	-0.67	0.28	0.99	-0.85
	Shediac Valley		-0.11	1.86	0.42	-0.74	-1.65	-0.16	0.22	0.17	-0.25	-0.46	-0.08
	Magdalen Shallows		-0.47	1.92	0.29	0.48	-1.15	0.22	-0.09	-1.19	-1.14	-1.75	-0.08
	Northeast Gulf of St. Lawrence		1.90	0.63	-0.08	-0.05	-0.65	-1.43	0.31	-0.64	-0.96	-1.30	0.25
	Cabot Strait		-0.41	-0.54	-1.59	1.72	0.54	-0.59	0.30	0.57	-1.12	-2.25	1.25
Mean surface Chl - September to December	Northwest Gulf of St. Lawrence		-2.03	-0.40	-1.02	-0.89	-0.90	-0.03	1.46	1.39	0.39	1.36	-0.97
	Anticosti Gyre		-2.11	-0.45	-0.66	-0.60	-1.11	-0.37	0.79	1.95	0.45	0.44	-1.70
	Shediac Valley		0.41	-0.74	-0.78	-1.13	0.17	-0.35	1.96	0.75	0.11	-0.98	-0.84
	Magdalen Shallows		-1.04	-0.90	0.21	-0.68	-0.33	-0.60	0.57	2.17	-0.45	0.87	-1.07
	Northeast Gulf of St. Lawrence		-0.54	-0.78	-0.72	-0.89	-0.08	-0.02	-0.49	1.02	1.95	-1.12	-0.88
	Cabot Strait		1.23	-1.01	-0.38	-1.67	0.74	-0.10	0.45	0.53	1.42	-0.72	-0.76

Indices of change in seasonality based on MODIS twice-monthly ocean colour composites

Index	Subregion	2002	2003	2004	2005	2006	2007	2008	2009	2010	2011	2012	2013
Start of spring bloom	Northwest Gulf of St. Lawrence		0.76	0.76	0.00	0.00	0.00	0.76	0.00	-2.29	0.00	-0.76	0.00
	Anticosti Gyre		1.35	0.75	0.15	0.15	-1.05	0.75	-0.45	-1.65	-2.25	-1.65	-1.05
	Shediac Valley		0.70	0.70	-0.90	0.70	-0.90	0.70	0.70	-1.70	-0.90	-0.90	0.70
	Magdalen Shallows		0.20	-1.37	-0.59	0.98	0.20	0.98	0.98	-1.37	0.20	-0.59	-0.59
	Northeast Gulf of St. Lawrence		1.58	0.00	0.00	-1.58	0.00	0.00	-1.58	-3.16	0.00	-1.58	-0.59
	Cabot Strait		0.98	0.20	0.20	-0.59	0.20	0.98	0.20	-2.15	-3.71	-1.37	-1.37
Timing of spring bloom peak	Northwest Gulf of St. Lawrence		1.21	1.21	-0.72	-0.72	0.24	0.24	0.24	-1.69	0.24	-0.72	0.24
	Anticosti Gyre		1.37	0.53	-0.32	-0.32	0.53	0.53	-0.32	-2.00	-1.16	-1.16	1.37
	Shediac Valley		0.78	-0.11	-1.89	-0.11	0.78	0.78	0.78	-1.00	-0.11	-1.89	-0.11
	Magdalen Shallows		0.47	0.47	-2.34	0.47	0.47	0.47	0.47	-0.47	1.40	-0.47	0.47
	Northeast Gulf of St. Lawrence		2.31	-0.10	-0.10	-0.10	-0.10	-0.10	-0.90	-0.90	0.70	-0.10	-0.10
	Cabot Strait		0.28	0.28	0.28	-0.85	0.28	1.41	0.28	-1.97	0.28	-1.97	0.28

Figure 18. Annual anomalies (scorecard) of chlorophyll biomass indices (means for various time periods and the magnitude of the spring bloom) and indices of seasonality (start and peak timing) of the spring phytoplankton bloom across Gulf of St. Lawrence statistical subregions from 2002 to 2013. The reference period used to compute annual anomalies was 2003–2010. Blue colours indicate anomalies below the mean and reds are anomalies above the mean.

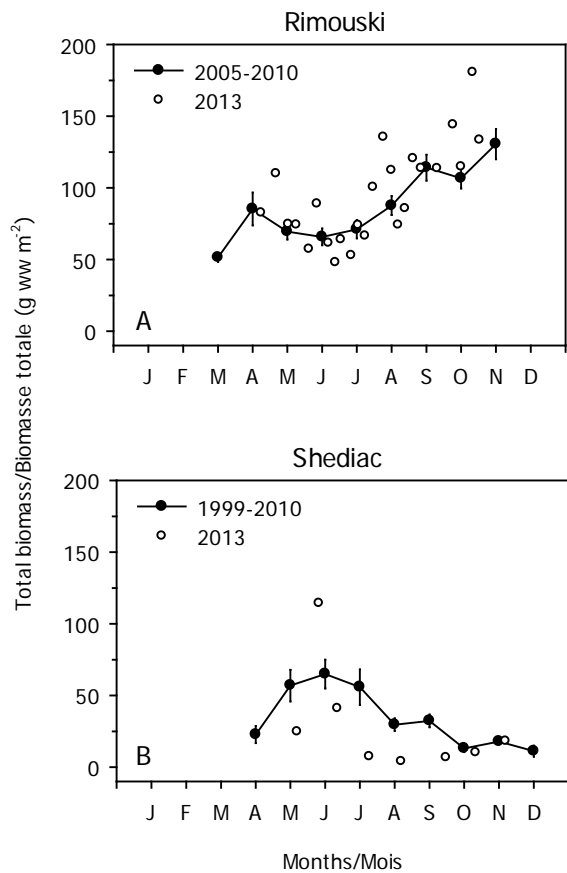


Figure 19. Comparison of total zooplankton biomass (based on wet weight) in 2013 (white circles) with the monthly climatology from Rimouski (A; 2005–2010) and Shediac Valley (B; 1999–2010) stations (solid lines). Vertical lines are standard errors of the annual averages.

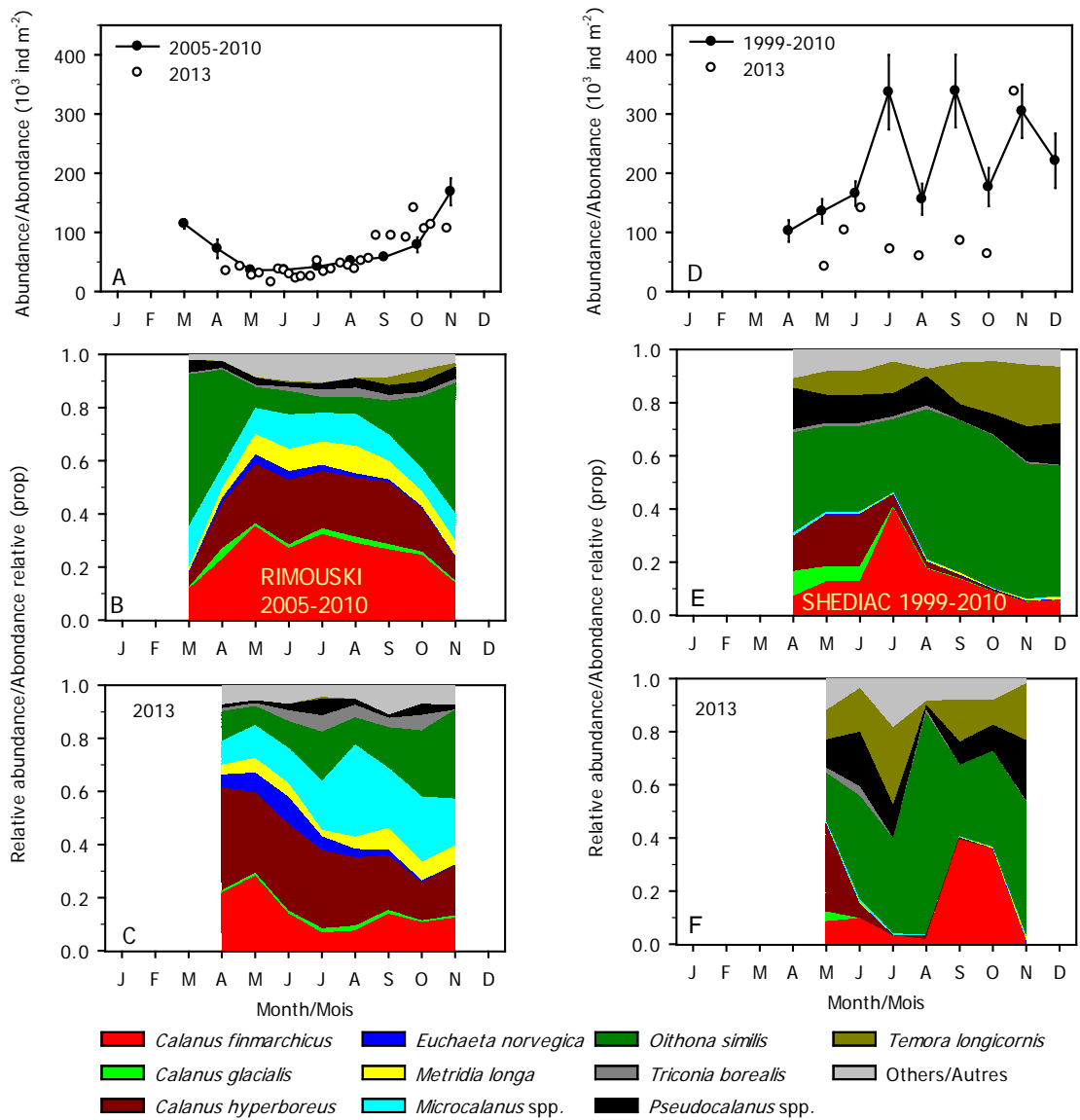


Figure 20. Seasonal variability in abundances of the 10 dominant copepod species at Rimouski (left panels) and Shediac Valley (right panels) stations. Climatologies of combined counts for the reference periods (solid lines) are plotted with data from 2013 (white circles) (including the “others” category; A, D). Seasonal variability by species for the reference periods (B, E) and 2013 (C, F) are also shown. Vertical bars in A, D are standard errors.

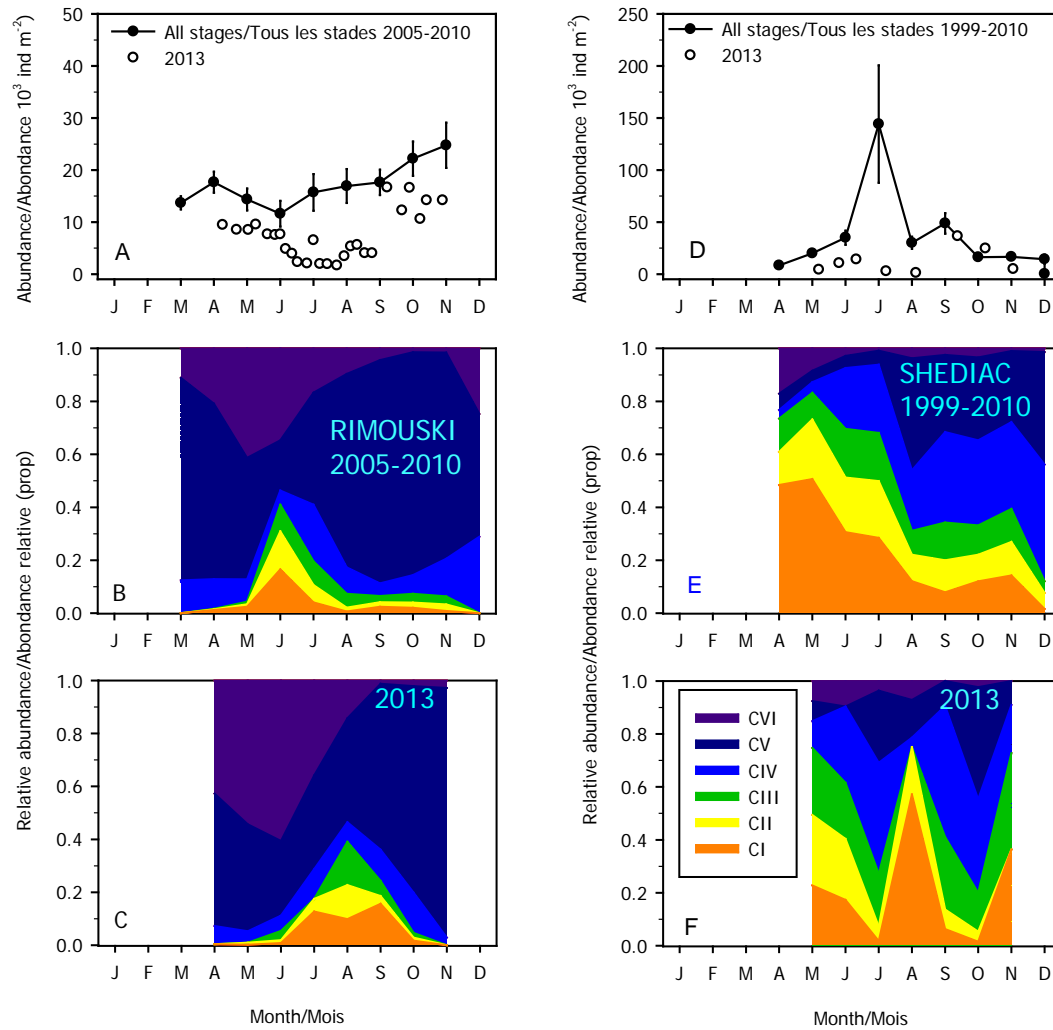


Figure 21. Seasonal variability in *Calanus finmarchicus* copepodite abundances at Rimouski (left panels) and Shediac Valley (right panels) stations. Climatologies of combined counts for the reference periods (solid lines) are plotted with data from 2013 (white circles) (A, D). Seasonal variabilities for the individual copepodite stages for the reference periods (B, E) and for 2013 (C, F) are also shown. Vertical bars in A, D are standard errors.

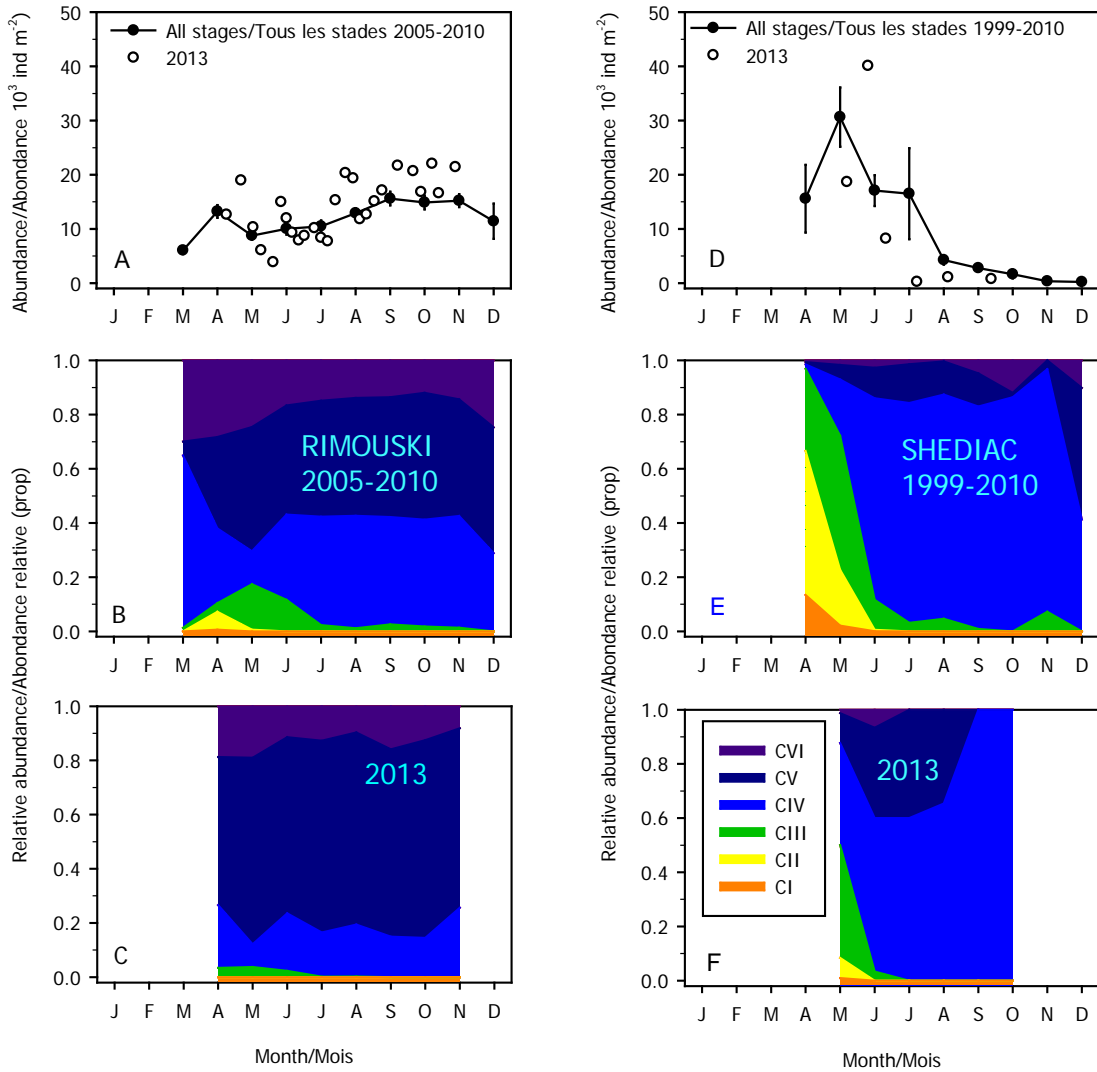


Figure 22. Season variability in *Calanus hyperboreus* copepodite abundances for Rimouski (left panels) and Shediac Valley (right panels) stations. Climatologies of combined counts for the reference periods (solid lines) are plotted with data from 2013 (white circles) (A, D). Seasonal variability for the individual copepodite stages for the reference periods (B, E) and for 2013 (C, F) are also shown. Vertical bars in A, D are standard errors.

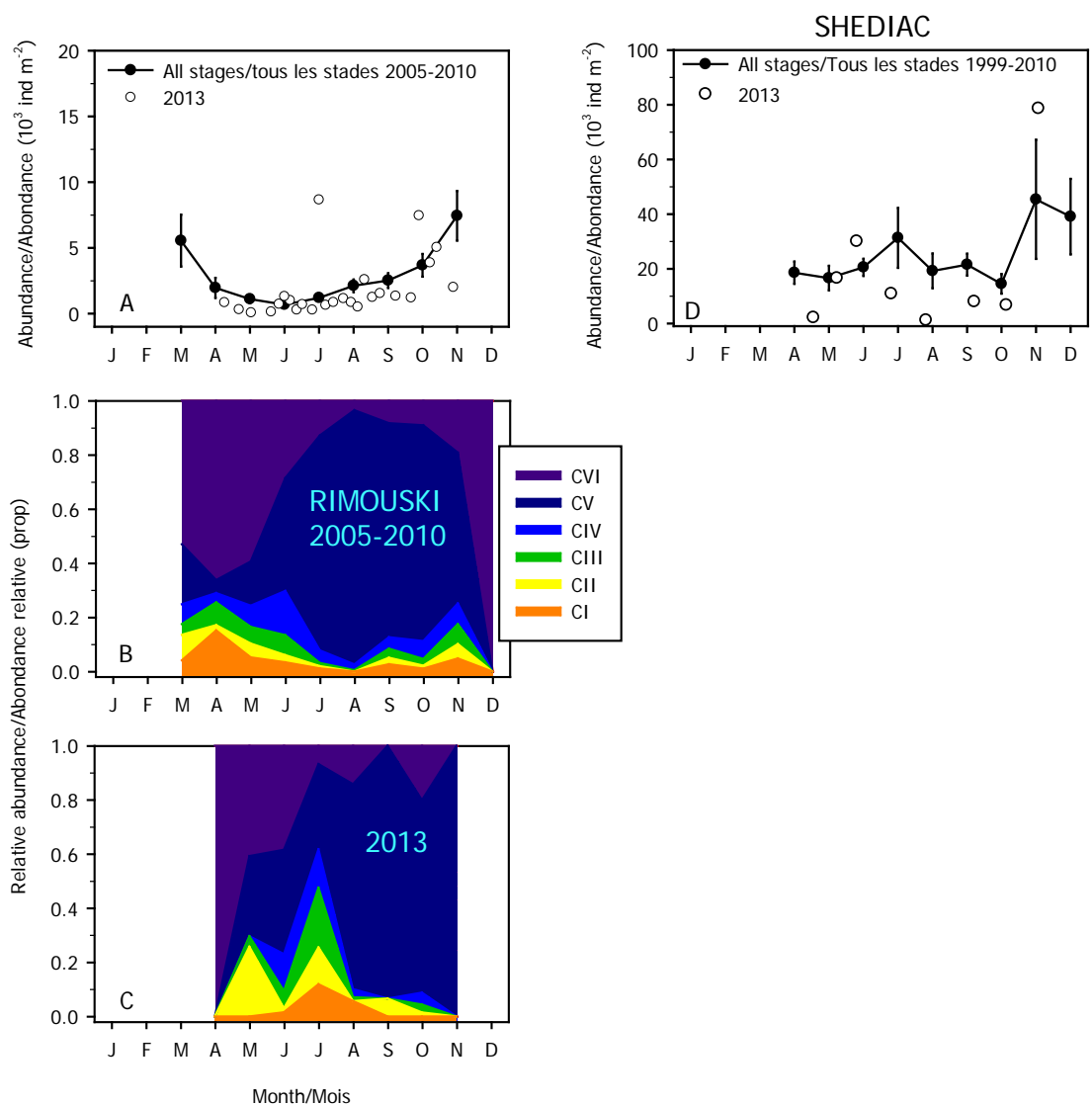


Figure 23. Season variability in *Pseudocalanus* spp. copepodite stage abundances for Rimouski (left panels) and Shediac Valley (right panel) stations. Climatologies of combined counts for the reference periods (solid lines) are plotted with data from 2013 (white circles) (A, D). Seasonal variability for the individual copepodite stages for the reference periods (B) and for 2013 (C) are also shown. Vertical bars in A, E are standard errors. No stage information is available for Shediac Valley station.

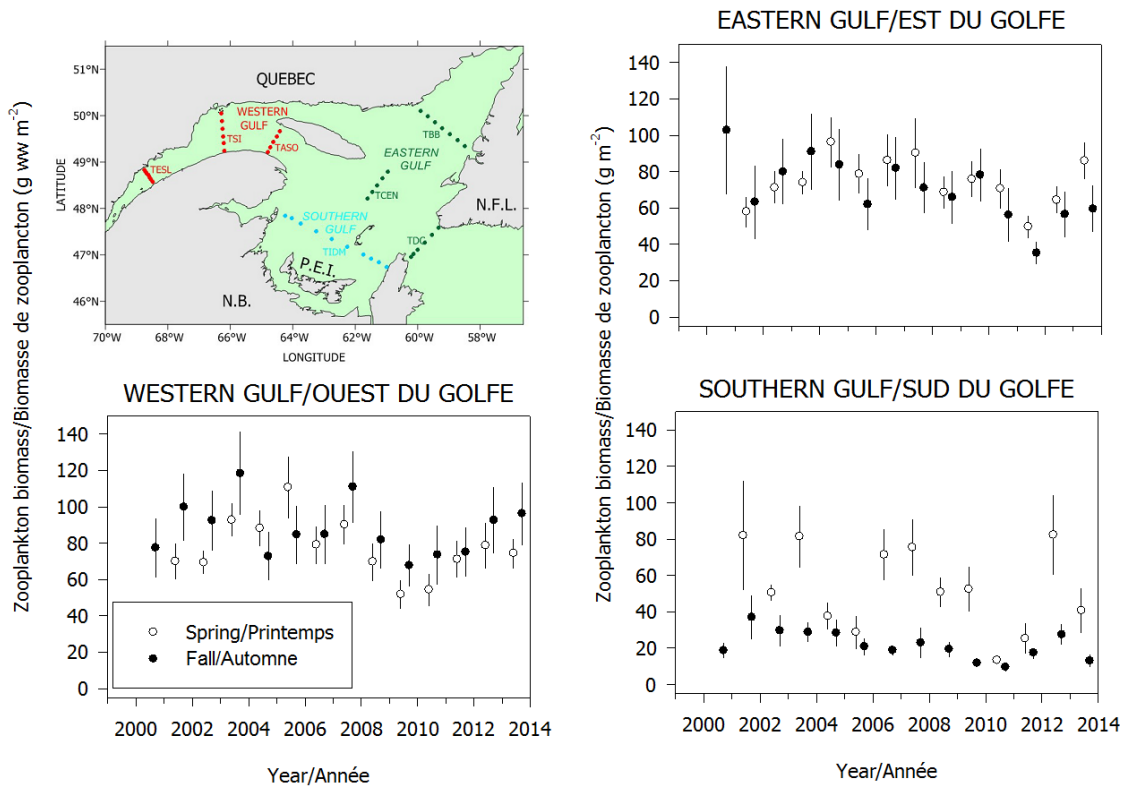


Figure 24. Mean total zooplankton biomass (based on wet weight) during spring and fall for three subregions of the Estuary and Gulf of St. Lawrence from 2000 to 2013. Vertical bars represent standard errors.

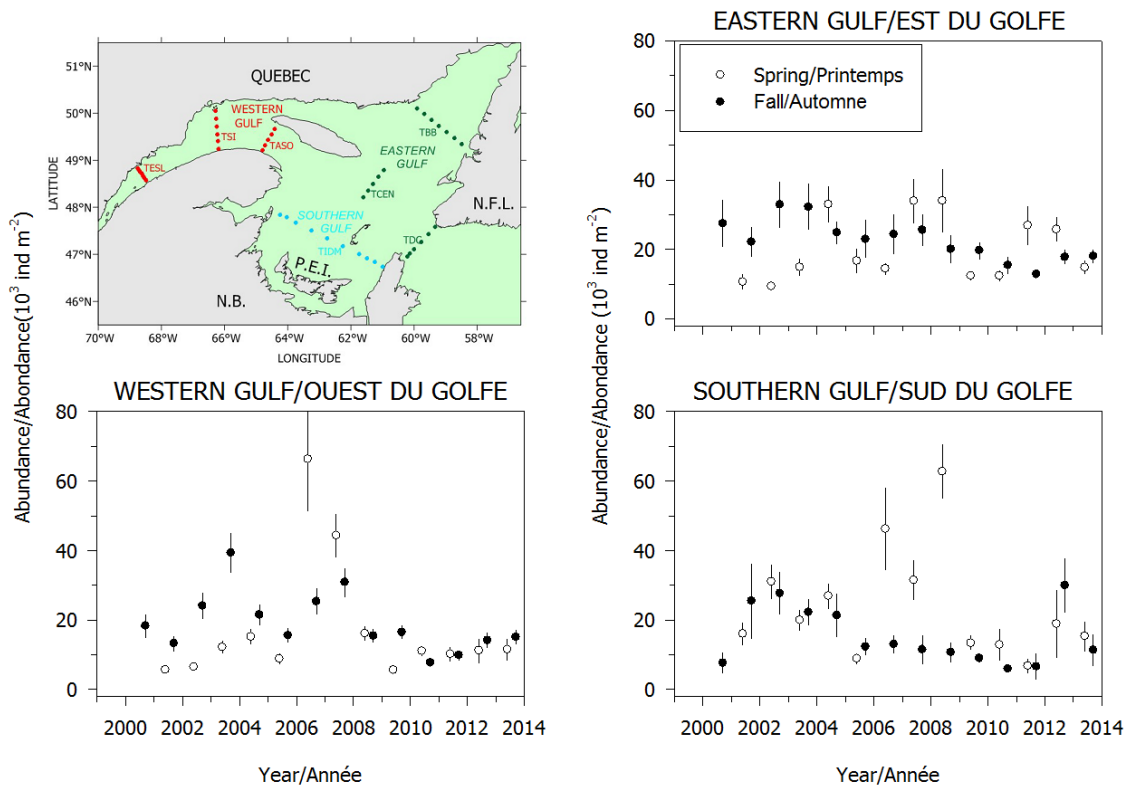


Figure 25. Mean total abundance of *Calanus finmarchicus* during spring and fall for three subregions of the Estuary and Gulf of St. Lawrence from 2000 to 2013. Vertical bars represent standard errors.

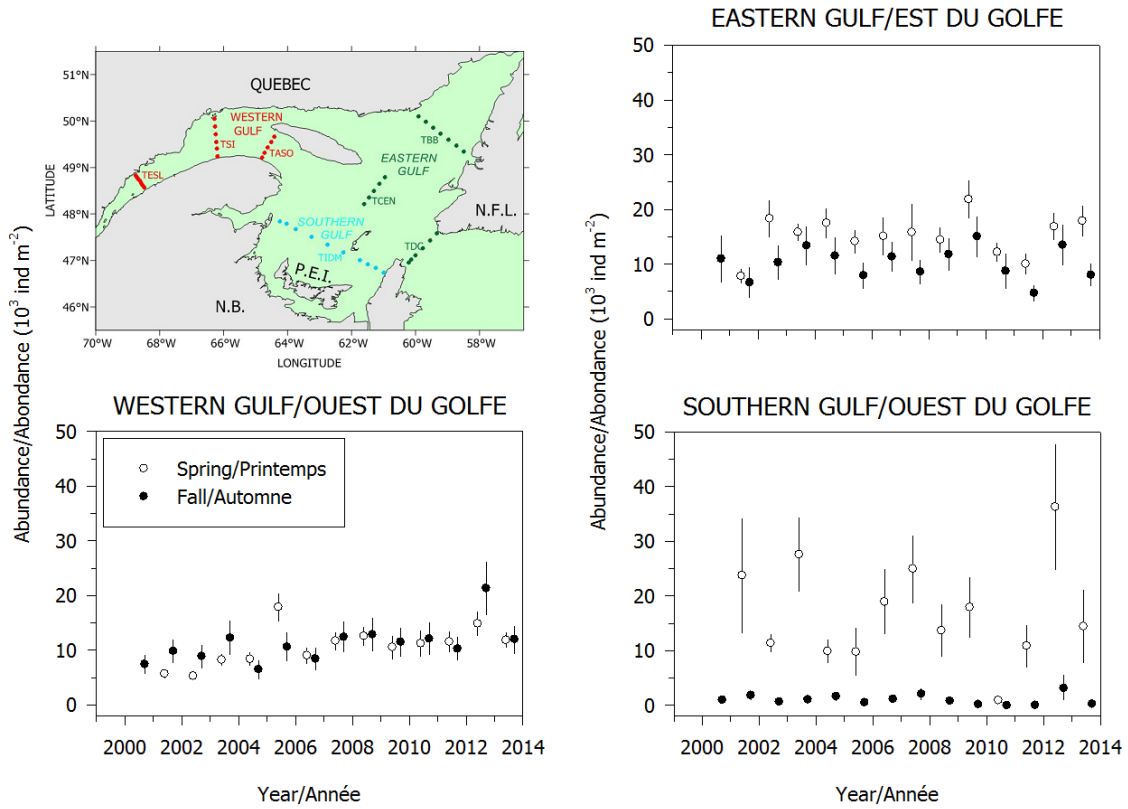


Figure 26. Mean total abundance of *Calanus hyperboreus* during spring and fall for three subregions of the Estuary and Gulf of St. Lawrence from 2000 to 2013. Vertical bars represent standard errors.

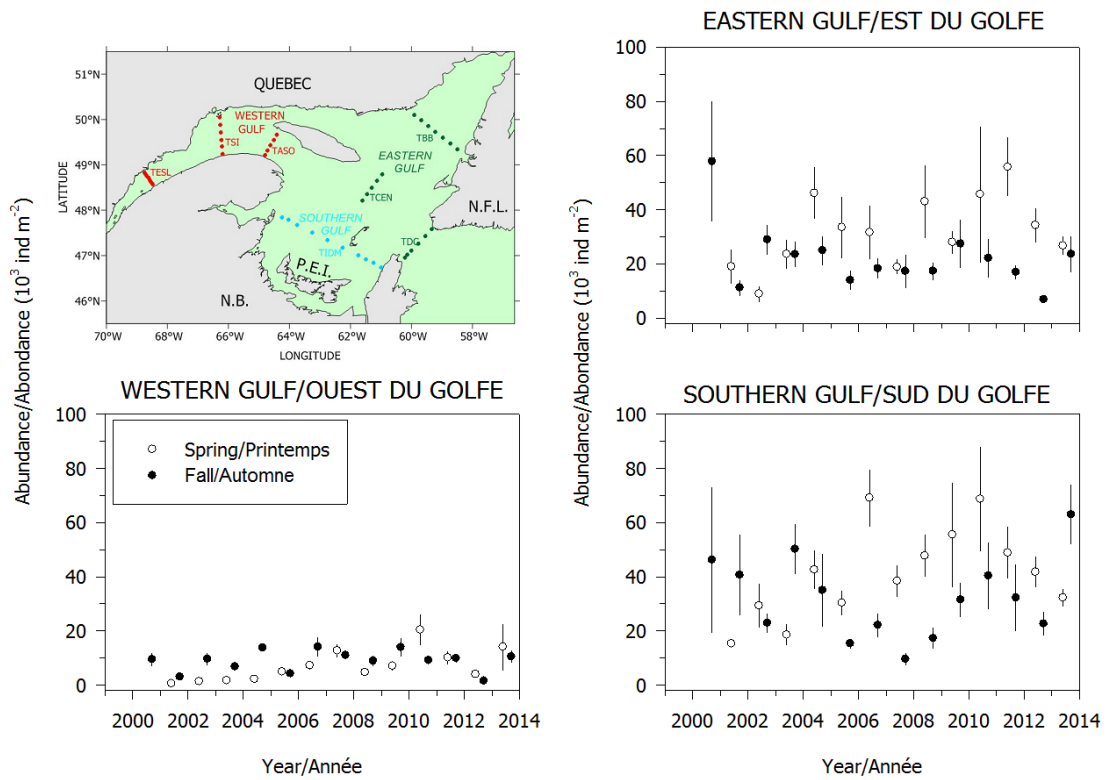


Figure 27. Mean total abundance of *Pseudocalanus* spp. during spring and fall for three subregions of the Estuary and Gulf of St. Lawrence from 2000 to 2013. Vertical bars represent standard errors.

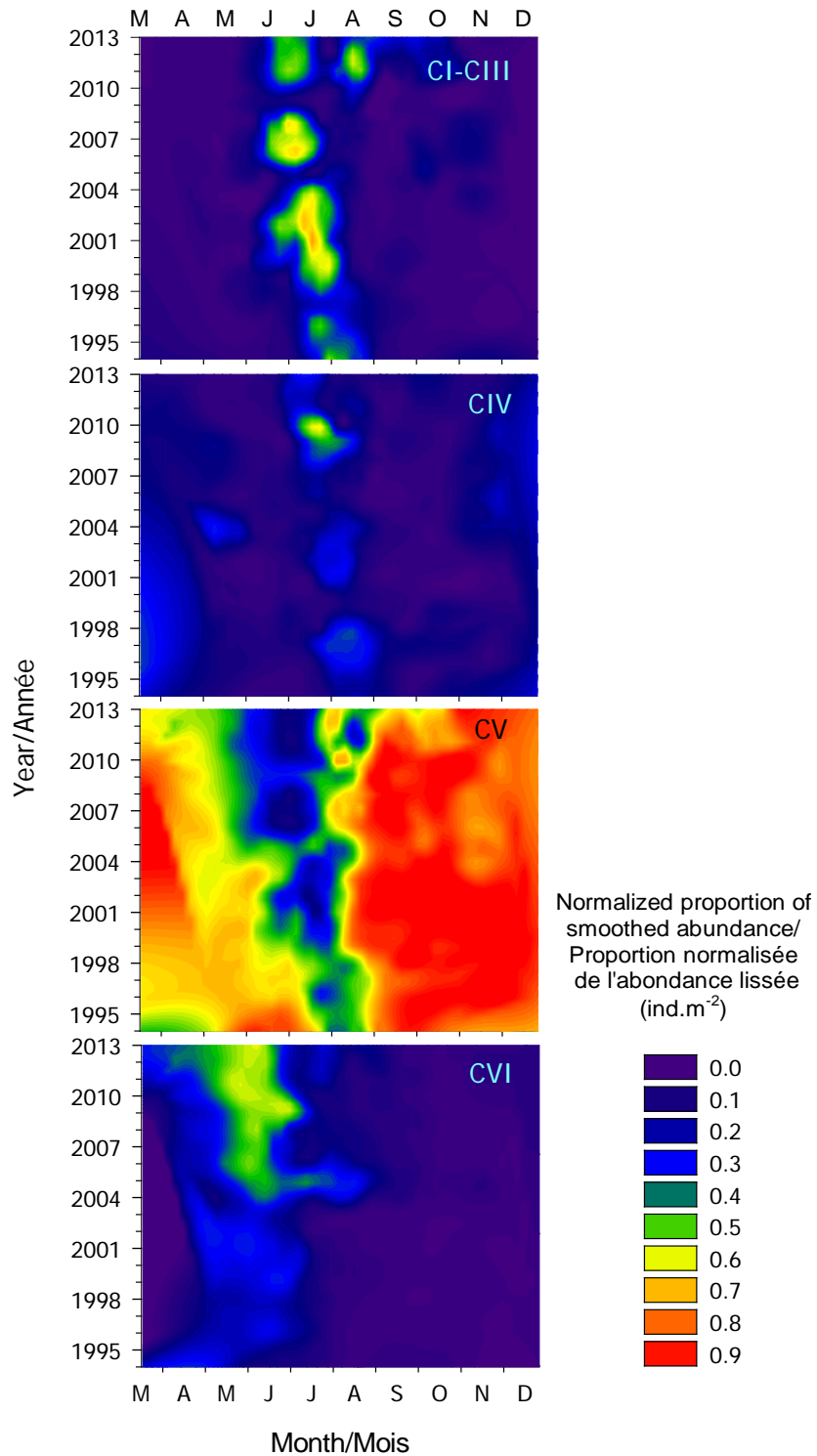


Figure 28. Seasonal cycle in relative stage proportions (percentage of total abundance) of stage CI–III, CIV, CV, and CVI (male + female) *Calanus finmarchicus* copepodites from 1994 to 2013 at Rimouski station.

	Region	1999	2000	2001	2002	2003	2004	2005	2006	2007	2008	2009	2010	2011	2012	2013
<i>C. finmarchicus</i>	Rimouski							-0.94	-0.03	1.78	0.30	-0.19	-0.91	-0.76	-0.58	-0.98
	Shediac	-0.56	-0.29	-0.19	-0.42	2.43	1.30	-0.61	0.22	-0.37	0.49	-0.98	-1.02	-0.96	-0.29	-1.12
	wGSL		-0.15	-0.87	-0.40	0.51	-0.17	-0.58	2.17	1.50	-0.36	-0.76	-0.90	-0.84	-0.61	-0.57
	sGSL		-1.38	0.50	0.91	0.04	0.38	-1.07	0.93	0.07	1.67	-1.01	-1.04	-1.48	0.38	-0.78
	eGSL		0.92	-1.06	-0.19	0.39	1.24	-0.44	-0.52	1.34	0.85	-1.08	-1.46	-0.37	-0.08	-1.01
<i>Pseudocalanus</i> spp.	Rimouski							-1.22	-0.42	0.68	-0.69	0.10	1.55	1.61	-1.14	-0.41
	Shediac	1.32	-0.93	1.93	-0.38	-0.38	-0.61	0.46	-1.47	-0.76	-0.42	0.41	0.84	2.18	-0.23	-0.46
	wGSL		0.39	-1.59	-0.64	-0.95	-0.14	-0.91	0.69	1.01	-0.30	0.66	1.77	0.53	-1.37	1.12
	sGSL		0.74	0.25	-1.02	-0.30	0.12	-1.32	0.69	-1.22	-0.47	0.51	2.01	0.24	-0.50	0.87
	eGSL		2.50	-1.11	-0.80	-0.40	0.70	-0.36	-0.27	-0.87	0.16	-0.05	0.50	0.73	-0.65	-0.27
Total copepods	Rimouski							-1.52	-0.72	0.94	-0.04	1.12	0.21	1.34	-0.42	-0.42
	Shediac	0.70	-0.93	-0.08	-0.40	0.09	-0.69	-0.33	-0.58	0.26	2.84	-0.56	-0.33	0.38	-0.53	-1.89
	wGSL		0.08	-1.65	-0.95	-1.15	-0.53	-0.21	1.42	0.42	0.88	0.43	1.25	-0.25	-1.43	-1.21
	sGSL		-0.66	-0.31	0.46	-0.75	-0.75	-1.79	1.00	-0.19	1.64	1.05	0.29	-0.02	0.21	-1.75
	eGSL		2.07	-1.99	0.07	-0.14	0.74	-0.84	-0.45	-0.02	0.37	-0.13	0.32	0.53	-0.67	-1.01
Non copepods	Rimouski							-0.95	-0.72	1.29	-0.96	0.47	0.88	1.88	-1.13	2.49
	Shediac	2.09	-1.10	0.64	-0.22	-1.18	-0.83	0.89	0.34	0.04	0.86	-1.00	-0.53	0.30	4.56	0.41
	wGSL		-0.63	-0.86	-0.81	-0.30	-0.74	-0.60	1.42	2.19	0.59	-0.14	-0.13	1.24	-0.26	-0.37
	sGSL		-0.67	-0.91	-0.27	-0.66	-0.76	0.52	-0.16	0.11	-0.06	0.17	2.70	1.94	1.73	2.38
	eGSL		-0.58	-1.44	-0.69	-1.14	0.26	1.68	1.25	1.10	-0.07	0.03	-0.42	4.37	-0.34	1.73

Figure 29. Normalized annual anomalies (scorecard) for four zooplankton categories at the high-frequency monitoring sites and the three subregions of the Estuary and Gulf of St. Lawrence (reference period: 1999–2010 [2005–2010 for Rimouski station]). Blue colours indicate anomalies below the mean and reds are anomalies above the mean.

	Region	1999	2000	2001	2002	2003	2004	2005	2006	2007	2008	2009	2010	2011	2012	2013
<i>C. hyperboreus</i>	Rimouski							0.80	-0.11	0.19	1.35	-1.21	-1.01	0.63	0.84	0.61
	Shediac	0.25	0.91	-0.54	-1.38	1.28	-0.84	1.52	1.11	0.04	-1.13	-0.65	-0.57	-1.04	2.52	-0.38
	wGSL		-1.09	-0.93	-1.25	0.16	-1.05	1.40	-0.54	0.91	1.19	0.47	0.72	0.40	3.51	0.81
	sGSL		-1.27	-1.07	-0.12	1.60	-0.13	-0.36	0.69	1.43	0.08	0.47	-1.32	-0.30	2.75	0.10
	eGSL		-0.94	-0.71	0.50	0.58	0.71	-0.93	0.06	-0.39	-0.02	2.28	-1.14	-2.46	0.84	-0.12
Small calanoids	Rimouski							-1.08	-0.74	0.16	-0.68	1.02	1.32	4.09	0.89	0.70
	Shediac	-0.91	-0.91	-0.83	-0.85	-0.84	0.11	0.32	-0.14	-0.10	0.47	1.60	2.07	4.56	0.32	2.08
	wGSL		-0.74	-1.23	-1.10	-1.12	-0.26	-0.52	1.27	0.68	1.08	0.78	1.15	0.93	-0.29	0.47
	sGSL		-0.83	-1.56	-0.51	0.13	-0.62	-0.54	1.16	-0.67	0.84	1.19	1.42	1.91	0.68	0.42
	eGSL		-0.97	-1.82	-1.10	0.21	1.04	0.28	0.34	-0.66	0.83	0.46	1.38	2.90	0.05	0.20
Large calanoids	Rimouski							-0.12	-0.10	1.65	0.51	-0.79	-1.16	-0.21	-0.35	-0.66
	Shediac	-0.31	0.18	-0.36	-1.11	2.48	0.71	0.27	0.49	-0.06	-0.03	-1.22	-1.04	-1.41	1.00	-1.35
	wGSL		-0.16	-1.01	-0.55	0.35	-0.39	0.00	2.00	1.71	-0.31	-0.89	-0.76	-0.81	-0.06	-0.60
	sGSL		-1.62	0.07	0.58	0.56	0.20	-0.98	1.01	0.65	1.44	-0.52	-1.39	-1.38	1.53	-0.63
	eGSL		0.64	-1.40	-0.46	0.24	1.11	-0.63	-0.43	1.66	0.64	0.16	-1.53	-1.15	0.75	-0.82
Cyclopoids	Rimouski							-1.15	-0.39	-0.37	-0.46	1.60	0.77	-0.39	-1.10	-0.42
	Shediac	1.03	-0.81	-0.04	-0.03	-0.72	-0.79	-0.13	-0.29	0.73	2.53	-0.73	-0.75	-1.27	-1.08	-2.22
	wGSL		0.17	-1.53	-0.82	-1.26	-0.44	0.07	0.78	-0.34	0.84	0.77	1.77	-0.45	-2.00	-1.59
	sGSL		-0.21	0.07	1.02	-1.70	-0.81	-1.53	0.14	0.83	1.36	0.66	0.19	-1.94	-0.60	-2.63
	eGSL		1.84	-1.98	0.43	-0.58	0.36	-1.00	-0.43	0.26	0.53	-0.12	0.71	0.19	-1.17	-1.27
Copepod: warm species	Rimouski							-0.65	-0.48	1.93	0.15	-0.01	1.23	8.29	0.63	6.99
	Shediac	2.06	0.37	1.71	-0.19	-0.14	-0.95	-0.78	-1.10	-0.82	0.28	-0.39	-0.05	-1.12	0.96	-1.22
	wGSL		0.62	-0.84	-1.04	-1.01	-0.91	-0.73	-0.42	0.84	1.74	0.82	0.93	2.51	0.62	4.11
	sGSL		-0.01	-0.70	-0.21	-0.52	-0.68	-0.61	-0.16	-0.55	-0.11	2.70	0.85	1.09	7.11	-0.26
	eGSL		2.40	-0.97	-0.74	-0.83	-0.77	0.30	0.30	-0.56	0.31	0.88	-0.33	2.98	3.76	0.29
Copepod: cold species	Rimouski							1.67	-0.12	-0.02	-1.29	-0.63	0.39	0.30	-0.87	-1.07
	Shediac	0.18	1.78	-0.06	-1.45	-1.15	-0.56	1.86	-0.35	-0.56	0.30	-0.19	0.20	-0.87	3.41	-1.13
	wGSL		-0.81	0.20	1.03	-0.88	0.19	2.09	-0.44	0.42	-1.03	-1.20	0.43	-0.58	-0.76	-1.62
	sGSL		-1.34	1.34	-1.19	-1.02	-0.52	0.45	-0.06	0.50	0.68	1.60	-0.46	-0.47	1.00	-0.66
	eGSL		-0.75	0.26	-1.04	-0.53	-0.68	-0.03	-0.75	2.36	-0.40	0.69	0.88	0.21	1.22	-0.24

Figure 30. Normalized annual anomalies (scorecard) for six categories of zooplankton assemblages at the high-frequency monitoring sites and the three subregions of the Estuary and Gulf of St. Lawrence (reference period: 1999–2010 [2005–2010 for Rimouski station]). Blue colours indicate anomalies below the mean and reds are anomalies above the mean. Small calanoids: mostly neritic species such as *Pseudocalanus spp.*, *Acartia spp.*, *Temora longicornis*, and *Centropages spp.*; large calanoids: mostly *Calanus* and *Metridia* species; cyclopoids: mostly *Oithona spp.* and *Triconia spp.*; warm-water species: *Metridia lucens*, *Centropages spp.*, *Paracalanus spp.*, and *Clausocalanus spp.*; and cold/arctic species: *Calanus glacialis* and *Metridia longa*.